NOISE REDUCTION IN CENTRIFUGAL COMPRESSORS USING HELMHOLTZ RESONATORS

BY

MAAZ FAROOQUI

A Thesis Presented to the

DEANSHIP OF GRADUATE STUDIES

KING FAHD UNIVERSITY OF PETROLEUM & MINERALS

DHAHRAN, SAUDI ARABIA

In Partial Fulfillment of the
Requirements for the Degree of

MASTER OF SCIENCE
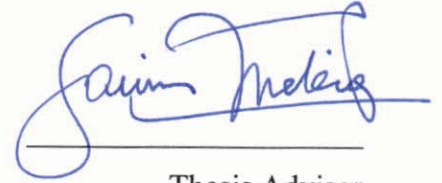
In

Mechanical Engineering

APRIL, 2012

KING FAHD UNIVERSITY OF PETROLEUM & MINERALS

DHAHRAN, SAUDI ARABIA

DEANSHIP OF GRADUATE STUDIES

This thesis, written by **Maaz Farooqui** under the direction of his thesis advisor and approved by his thesis committee, has been presented to and accepted by the Dean of Graduate Studies, in partial fulfillment of the requirements for the degree of **MASTER OF SCIENCE in MECHANICAL ENGINEERING**.

Thesis Committee

Thesis Advisor
Dr. Samir Mekid

Member
Dr. Muhammad A. Hawwa

Member
Dr. Hussain Al-Qahtani

Department Chairman
Prof. Dr. Amro M. Al-Qutub

Dean of Graduate Studies
Dr. Salam A. Zummo

29/5/12

Date

بِسْمِ اللهِ الرَّحْمٰنِ الرَّحِيْمِ

Dedicated to my mother, my mother, my mother, my father, my brother and my teachers

ACKNOWLEDGEMENTS

In the Name of Allah, the Most Beneficent, the Most Merciful.

Praise belongs to Allah, the Lord of all the worlds (2) The All-Merciful, the Very-Merciful. (3) The Master of the Day of Requital. (4) You alone do we worship, and from You alone do we seek help. (5) Take us on the straight path (6) The path of those on whom You have bestowed Your Grace, Not of those who have incurred Your wrath, nor of those who have gone astray. (7)

Al-Fatiha

I begin with the name of Allah, the most beneficent, the most merciful. May Allah bestow peace on our beloved Prophet Mohammed (*peace and blessings of Allah be upon him*), and his family. I would not have able to complete this work without the help of Allah who endowed me with health, courage, aptitude and patience.

During this work my parents were a constant source of motivation and support. Their prayers, love and encouragement helped me to arrive at this milestone. I would like to thank my teacher Dr. Abid Halim. The things I learnt from him are some of the most important lessons of my life.

Acknowledgements are due to *King Fahd University of Petroleum and Minerals* which gave me the opportunity to pursue a graduate degree and also for all the support I received in carrying out this research. I am also grateful to the *Dresser Rand* at *KFUPM* (ME project # 002351) and *Saudi Aramco* for its support during this research.

I would like to express my gratitude to my thesis advisor Dr. Samir Mekid for all he taught me, for his patience when I couldn't get things done and for his help when I

Table of Contents

LIST OF TABLES

LIST OF FIGURES

ABSTRACT (ENGLISH)

NAME:	Maaz Farooqui
TITLE:	Noise Reduction in Centrifugal Compressors using Helmholtz Resonators.
MAJOR FIELD:	MECHANICAL ENGINEERING
DATE OF DEGREE:	APRIL 2012

Compressors are at the heart of most petrochemical and industrial power plants. These plants require fluids at high energy (High pressures and velocities), and due to this requirement compressors are used as the primary means of raising the fluid to a higher energy state.

Of the various types of compressors, centrifugal compressors are most commonly used in Saudi Arabia due to their continuous flow operation and moderation head capacity. Despite their common usage, centrifugal compressors are often major noise generators due to their high horsepower and high tip speeds. This noise is undesirable for people living close to installation and also can potentially cause structural failures in the piping. Particular attention is given to the modified solution using the Helmholtz Resonator concept. A comparison of the noise reduction results between the developed solution and the existing solution is made. A thorough numerical simulation of acoustic wave propagation for one and two degrees of freedom Helmholtz resonators is presented and is validated with experimental results from the available literature. The calculated resonant frequencies for different geometries of one and two degrees of freedom resonators agree well with the experimental results .The effect of end-correction factors has also been incorporated in this study. The results from published papers are reproduced and validated using COMSOL, FEM based software.

Attention is also given to the effect of geometry shape of the Helmholtz resonator on its resonant frequency and on its noise attenuation capability. The theory of resonant frequency depending on the shape of the vessel of the resonator is verified numerically using COMSOL. The Numerical simulation is supported with an experimental validation too. Some new configurations of the resonator arrays are also simulated and presented with significant improved results in comparison to those already in practice.

ABSTRACT (ARABIC)

ملخص الرسالة

الاسم: معاذ فاروقي

عنوان الرسالة: الحد من الضوضاء في ضواغط الطرد المركزي باستخدام الهيلمهولز ريزينيتور.

التخصص:الهندسة الميكانيكية

تاريخ التخرج: 1434 هـ - (ابريل 2012 م)

الضواغط هي في صميم معظم محطات توليد الطاقة البتروكيميائية والصناعية . هذه المحطات تحتاج الى موائع تستخدم بوجود طاقة عالية (ضغوط وسرعات عالية)، و بسبب هذه الشروط ، الضواغط تستخدم كوسيلة اساسية لزيادة المائع الى اعلى حالة طاقة.

من الانواع المختلفة من الضواغط ، ضواغط الطرد المركزي والتي هي الاكثر استخداما في المملكة العربية السعودية وذلك بسبب عملها المستمر في التدفق والاعتدال بقدرة الراس . بالرغم من الستخدام الشائع ، ضواغط الطرد المركزي مولد رئيسي للضوضاء بسبب قدرتها وسرعاتها العالية.

هذا الضجيج غير مرغوب للناس الذين يعيشون على مقربة من مناطق استخدام ضواغط الطرد المركزي, و يمكن ان تتسبب في انهيار التركيب الهيكلي للانابيب . ويولى اهتمام جزئي لتطوير حل لهذه المشكلة وذلك عن طريق استخدام مفهوم اله يلمهولز ريزينيتور . تم اجراء مقارنة بين نتائج تخفيض الضوضاء عن طريق الحل المطور والنتائج الموجودة مسبقا . و تم عرض محاكاة رقمية لانتشار الموجات الصوتية باستخدام هيلمهولز ريزينيتور واحد وايضا باستخدام اثنين وبالاضافة الى ذلك تم التحقق من صحة النتائج بمقارنتها بدراسات عملت سابقا. الترددات الرنانة المحسوبة لمختلف الاشكال الهندسية باستخدام هيلمهولز ريزينيتور واحد وايضا باستخدام اثنين تتوافق بشكل حسن مع النتائج التجريبية. تأثير نهاية تصحيح العوامل ايضا تم دراسته . تم التحقق من النتائج الماخوذة من الابحاث المنشور باستخدام بنامج الكومسول.

ويرد ايضا الانتباه الى تاثير الشكل الهندسي للهيلمهولز ريزينيتور عند ترددها الرنان وعلى قدرتها على تخفيض الضوضاء . تم التحقق رقميا باستخدام الكومسول من نظرية التردد الرنان بالاعتماد على شكل وعاء الرنان . المحاكاة الرقمية دعمت باستخدام ا لنتائج التجريبية . بعض التكوينات الجديدة من مصفوفات الرنان ايضا عرضت مع تحسين النتائج الهامة مقارنة بما سبق من الناحية العملية

CHAPTER 1

INTRODUCTION

Compressors have been identified as major noise sources, and this is understandable. Large numbers of compressors, of all types, are used in refineries, chemical plants, generating stations, and other major industries. Certain types of compressors generate relatively high noise levels even above those permitted by the Occupational Safety and Health Act, and therefore need attention[12] In many developed countries, such as United Sates, France, Germany and Australia, governments have stepped in to protect citizens from this aural assault with regulations that set maximum sound levels for machineries, vehicles, and airplanes. Switzerland has gone so far as to prohibit aircraft departures between 11:30 p.m. and 5:00 a.m., except in unusual and unforeseen cases. The problem has also found its way into the Saudi Arabian industrial areas.

Huge amount of noises is generated from the rotating equipments and machineries especially from the centrifugal compressors used in a number of refining units of Saudi Aramco. These circumstances create problems for the employees working in some of the refineries such as they are unable to hear the fire and safety alarms, due to the high

intensity of noise generated by the compressors. They are prone to hearing impairment, hypertension, vasoconstriction and other cardiovascular impacts.

It is obvious that compressor sound control is needed, and this requires an understanding of the noise generating process. Various techniques have been found to be effective in reducing the noise of centrifugal, axial, and reciprocating compressors. The biggest impact of this noise is the discomfort of the personnel working at the facility as observed in practice. The noise levels in compressors vary over a wide range from 70 – 120 dBA [1, 2, 3]. As the compressor operates over its lifetime, the noise and vibration levels expectedly increase, since centrifugal compressors are continuous flow machines and are extensively used in Saudi Arabia at crude oil processing facilities such as Saudi Aramco, maintenance is periodic and stopping the operation every time noise levels exceed the desired threshold can be very expensive.

This imperilment can be subdued by following noise reduction procedures. Noise Reduction can be achieved by two different methods. The first one consists of using passive means which are based on the absorption and reflection of noise and has excellent noise cancellation properties for frequencies above 1 KHz. The other method consists of using active means, which can show considerable noise cancellation performance for noise frequencies below 1 KHz.

In this work I tried to explore these methods of noise reduction and come up with a practical add on solution to this menace. The development of an efficient noise attenuator is not just a benefit for the employees working around it. Quiet, smooth running

machines, or industrial processes, provides a commercial edge over competitors, and enables customers to fulfill stringent regulatory conditions. It enhances communication, improves transfer of instructions, improves efficiency, enhances safety, and minimizes hearing losses. It is not something which can't be ignored and its urgent need and the numerous benefits behind it call for its proper and timely implementation in each and every industry suffering noise hazards.

1.1 BACKGROUND

Sounds consist of pressure waves. The intensity of sound is known as the sound pressure level, or in short SPL. The human ear can detect a wide range of sound pressure levels. Sounds can be very soft, such as the ticking of a wristwatch, or very loud, such as a top fuel dragster doing a burnout. The intensity of sound pressure can be measured, and is expressed as decibels, or dB. Alexander Graham Bell founded the concept of decibels and formulated a logarithmic scale based on 10. "Deci" refers to the base 10 log scale, and "Bel" refers to Alexander Bell.

Figure 1.1 shows some sources of noise for comparison purposes. It can be seen that 120 dB is equivalent to the sound of an airplane on the runway. This level of noise barely lies below the Human Pain Threshold and may lead to permanent and irreparable damage, especially with consistent exposure over long periods of time. Above 120 dB is the threshold of pain and human ear is unable to sustain noise at that frequency Fig 1.2
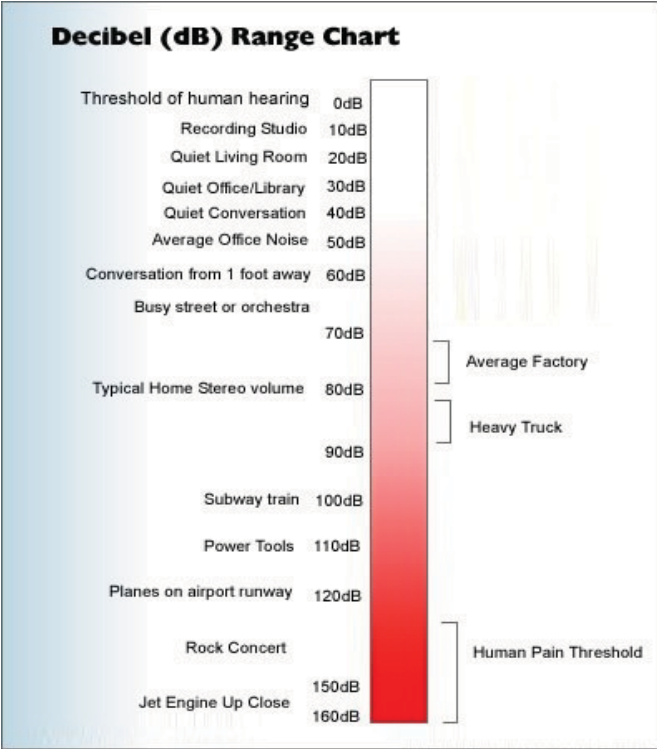
Figure 1.1 Chart displaying a comparison of Noise levels [55]
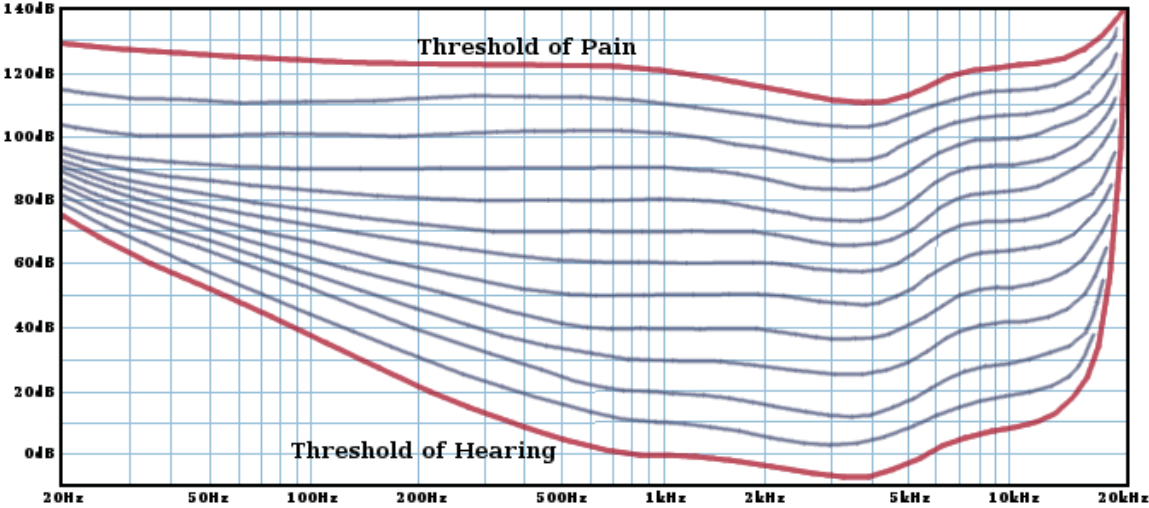
Figure 1.2 Chart displaying a comparison of Noise levels with frequency [56]

1.2 WAVE EQUATION

Sound waves in a lossless medium are governed by the following equation for the acoustic pressure, p (SI unit: Pa):

$$\frac{1}{\rho c^2}\frac{\partial^2 p}{\partial t^2} + \nabla\cdot\left(-\frac{1}{\rho}(\nabla p - q)\right) = Q \tag{1.1}$$

where ρ refers to the density, and c denotes the speed of sound. The dipole source **q** and the monopole source Q are both optional. The combination ρc^2 is called the adiabatic bulk modulus, commonly denoted by k In terms of acoustic potential function φ the wave equation can also be written in the form [33, 34]

$$\nabla^2\phi = \left(\frac{1}{c^2}\right)\frac{\partial^2\phi}{\partial t^2} \tag{1.2}$$

1.2.1 Plane Waves

For the case of plane wave propagation, only one spatial dimension, x, the direction of propagation is required to describe the acoustic field. An example of plane wave propagation is sound propagating along the center line of a rigid wall tube. In this case, Eqn. (1.2) written in terms of the potential function φ reduces to,

$$\frac{\partial^2\phi}{\partial x^2} = \left(\frac{1}{c^2}\right)\frac{\partial^2\phi}{\partial t^2} \tag{1.3}$$

5

1.3 SOUND FIELDS

In order to predict or model noise from equipment we need to understand, or better, define the sound fields and the predicted sound level associated with those fields. The near field, far field, free field and reverberant field are the most common. The regions that describe the sound fields and sound propagation are illustrated in Fig 1.2.
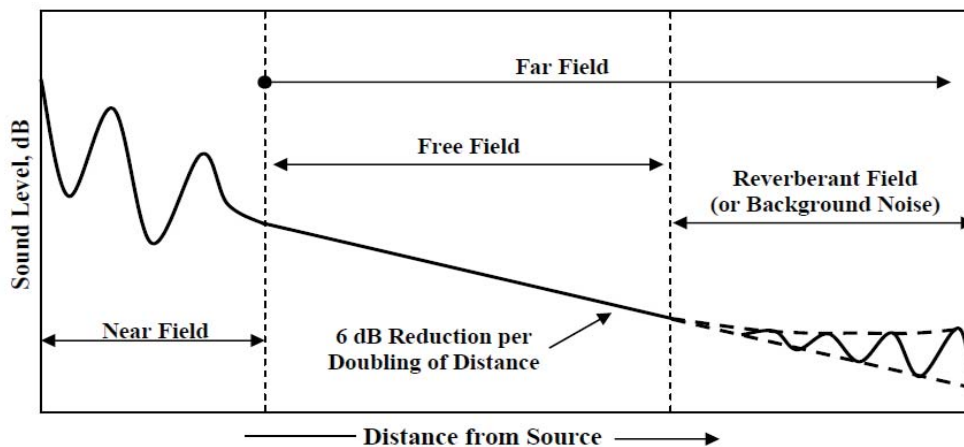
Figure 1.3 Definition of Sound Fields

The near field region is probably the most difficult to predict as this describes the region where noise propagation is not well developed and construction techniques and equipment installation details that are generally unknown This affect the amount of noise around the equipment or structure. The far field starts where the sound field becomes more stable and propagation is fairly uniform. This location is frequency (wavelength) dependent and is usually two to four major source dimensions (width and height as you look at the source) away from the noise source. The free field describes where sound

freely propagates and spreads uniformly. The sound level decreases approximately six decibels for every doubling of distance. As you get farther away from the source the decay rate starts to flatten out once the sound from the source approaches the ambient or background sound level as illustrated in the right section of the Fig 1.2. The reverberant field occurs where freely propagating sound waves are reflected back from a wall, a ceiling, or other surfaces again causing variation in sound levels as illustrated.

1.4 PROPAGATION MODELING OF SOUND

The radiation of sound comes from various sources: the aero/fluid-dynamic path from a fan, engine, turbine or flow regulating device; or, from the structural path from the engine body, duct wall, pipe wall, valve body, or enclosure wall. The radiation of sound may be generally described (modeled) by the following expression [57],

$$L_p = L_w + 10 Log\left(\frac{Q}{4\pi r^2}\right) - \sum A_i, dB - re : 20\mu Pa \tag{1.4}$$

Here re: 20μ Pa refers to the reference pressure taken for the calculations. This method is also commonly referred to as *ray tracing*, that is, the sound ray (path) is modeled by a set of geometric terms (Q/4πr2) and losses (ΣA_i) . Eqn (1.1) is the basic form and predicts the sound level L_p at a distance r (meters), where Q defines the reflective surfaces that are around the source of noise having a sound power, *Lw*. ΣA_i is the term used to account for all the elements that can affect the sound level (directivity, atmospheric loss, barriers, ground effects, trees, etc.).

Absent from Eqn. (1.4) is the functional descriptor for frequency. This expression is applied for each frequency band of interest. Each source of noise may have up to ten octave bands or up to 27 one-third octave bands. Eqn. (1.4) is applied to each band, and the overall sound level determined from the all the octave or one-third octave band sound pressure levels.

Q accounts for the reflective planes that bound the source of noise. These planes act as reflectors focusing the sound or bounding the sound to a certain area. It is also referred to as the solid angle of propagation (D_Ω) and by other descriptors.

Directivity of a specific nature may be introduced if known which is a measure of the sound level relative to the averaged sound level in a given direction and is called the Directivity Index,

$$DI_\theta = L_{p\theta} - \overline{L_p} dB \tag{1.5}$$

Where, L_p is the predicted or averaged sound level at the distance r versus the measured sound, $L_{p\theta}$. This enables the use of a specific Directivity Index applicable to the source of noise in order to predict sound levels from the source in a specific direction. Directivity is critically important

Sound measurements are most commonly done in Sound Pressure Levels (DB)., which can be defined as [35],

$$L_p = 10Log_{10}\left(\frac{p^2}{p^2_{re}}\right)[dB] \hspace{4cm} (1.6)$$

Where,

p= root mean square (rms) sound Pressure (Pa)

p_{re}=international reference pressure of 2.0 x 10^{-5} Pa

Eqn.(1.6) can also be written in a simpler form which is

$$L_p = 20Log_{10}p + 94[dB(re:2.0x10^{-5}Pa)] \hspace{3cm} (1.7)$$

1.5 MOTIVATION BEHIND PRESENT WORK

In this work I tried to explore these methods of noise reduction and come up with a practical add-on solution to this menace. The development of an efficient noise attenuator is not just a benefit for the employees working around it. Quiet, smooth running machines, or industrial processes, provides a commercial edge over competitors, and enables customers to fulfill stringent regulatory conditions. It enhances communication, improves transfer of instructions, improves efficiency, enhances safety, and minimizes hearing losses. It is not something which can't be ignored and its urgent need and the numerous benefits behind it call for its proper and timely implementation in each and every industry suffering noise hazards.

1.6 OBJECTIVES OF THIS WORK

The objectives of the thesis study are listed below:

1)   Design of One and Two Degree of freedom Helmholtz resonators for maximum possible noise reduction in ducts and pipelines based on real plant configuration.

2)   Study of geometry effects on the resonant frequency of the Helmholtz Resonators.

3)   Experimental, analytical as well as numerical validation of the designed resonators.

4)   Study of the behavior of a non homogeneous array of Helmholtz Resonators on noise reduction.

CHAPTER 2

LITERATURE REVIEW

2.1 SOURCES OF NOISE IN COMPRESSORS

Noise originates from various sources within compressors. The most critical source of noise in centrifugal compressors is considered to be the blade passing frequency. This noise arises from the interaction between the impeller blade and the stationary diffuser vanes [1,2,3]. It is widely known that Blade Passing Frequency (BPF) noise components come from the circumferential flow distortions upstream and downstream of the impeller [4]. The interaction between the impeller blades as it passes by the stationary diffuser vane causes a pressure pulsation which leads to the development of vortices.
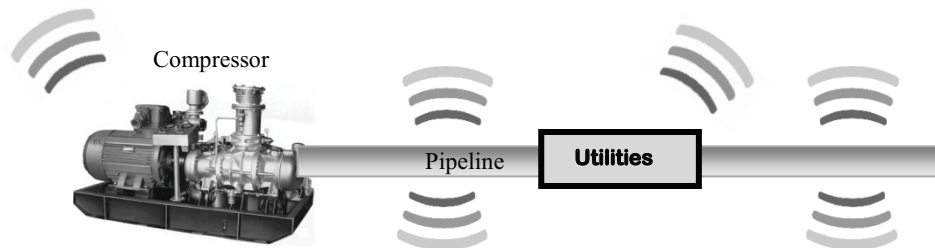
Figure 2.1 Source of Noise in compressor line

The interaction of these vortices as they move along the flow path creates the discrete frequency noises of the Blade Passing Frequency. Conventionally the BPF falls between 1000 Hz to 4500 Hz, usually depending on the speed of the compressor and the number of impeller blades [1]. This range falls within human hearing sensitivity which adds to the irritating nature of this noise. Although the BFP may be considered to be the most annoying aspect of compressor noise, at supersonic flow conditions another source of noise arises in the form of buzz saw noise. The BPF noise and the buzz saw noise coupled together can lead to structural failure due to fatigue especially at pipe nipples, stubs, and instrumentation connections.

In any centrifugal compressor as the fluid flow exits the impeller, the flow distribution is distorted. Specifically, such distorted flow is characterized by a low angle (relative to a tangent to the impeller circumference) fluid flow exiting most prominently adjacent to the shroud side of the diffuser. In the past, this distorted flow has been shown to cause severe compressor performance problems [5]

Due to the design of the compressor, the inlet and discharge pipes are relatively more susceptible to noise transmission that the compressor casing itself. Noise propagates through the medium of least resistance and since the piping at the inlet has thinner walls when compared to the compressor casing, this provides a path of lower resistance for noise propagation. Between the inlet and the discharge, investigations have found that higher vibration and noise levels emanate from the discharge. At the inlet the primary

source of noise is the rotor-alone noise, while at the diffuser the BPF noise is dominant [2].

Some other sources affecting the noise produced by the compressors are turbulence which produces noise using a combination of two affects i.e. Vortex shedding, and upstream turbulence. Increasing the radial distance between impeller blades and diffusers reduces noise. Rotational speed also has a definite effect on noise. For any particular design, the sound level will increase anywhere from 20 to 50 times the logarithm of the speed ratio. Another point that cannot be missed is the number of stages of the compressor. The noise generated by centrifugal compressors can be reduced by decreasing the work per stage that is, by increasing the number of stages. Head-capacity operating point also plays a very important role in the noise generation phenomenon in the centrifugal compressor. Mass flow and discharge pressure both have a profound effect on the noise produced by a compressor. As the mass flow is reduced the noise decreases until a point near surge is reached. Beyond this point the noise increases rapidly.

2.2 ACOUSTIC PREDICTION

Sound propagation in a duct with a uniform flow has been investigated by researchers [37-41] and they have presented a theoretical development, accompanied by an experimental check, of the attenuation in acoustically lined ducts with no flow. Fischer and Anderson [43] have investigated sound attenuation in a lined rectangular duct

without flow. The case of a duct carrying shear flow also has been investigated thoroughly to check for a solution of noise reduction due to the flow [44-53]

It is proved already that the dipole due to the unsteady pressure fluctuation is the dominant source of the centrifugal compressor noise. The most prominent source of the dipole in the centrifugal compressor is the rotating impeller. FW–H equation of the point dipole assumption is used to define the noise source of the centrifugal compressor impeller where $p(x, t)$ is the acoustic pressure, x is the observer position vector, t is the observer time, Cos ϴ is the directivity factor, f is the source strength, ω is the radiated frequency, r is the distance between the source and the observer point, and c is the speed of sound. The near- and far-field components are seen explicitly as $1/r^2$ and $1/r$ terms, respectively. [35]

$$p(x,t) = \frac{cos\theta f}{4\pi} \left\{ \frac{i\omega}{rc} + \frac{1}{r^2} \right\} e^{i\omega}(t - r/c) \qquad (2.1)$$

2.3 NOISE REDUCTION TECHNIQUES

Noise reduction techniques fall under three broad categories: Primary noise reduction, Secondary noise reduction and Tertiary noise reduction. Primary noise reduction involves reducing noise at the source; this usually means a complete redesign of the component or an add-on solution within the compressor itself. Secondary solutions include externally blocking noise; acoustic lagging, sound insulation, sound enclosures and sound reduction

in transmission are some examples. Tertiary solutions are solutions based on blocking noise on the receiving side, these can be in the form of ear plugs or some kind of ear protection for the personnel working around the facility. Normally in most industrial environments either tertiary or secondary noise reduction solutions are employed [2].

Device	Mechanism	Effective frequency range	Critical Dimension		Dependence of Performance on end conditions
			$D = fl/c = l/\lambda$		
			Length	Width	
1. Lumped	Suppressive	Band	D<1/8	D<1/8	Critical
2. Side Branch resonator	Suppressive	Narrow Band	D<1/4	D<1/8	Critical
3. Transmission Line	Suppressive	Narrow Band	D>1/8	D<1/4	Critical
4. Lined Duct	Dissipative	Broadband	Unbounded		Slightly Dependent
5. Lined Bend	Dissipative	Broadband	D>1/2	D>1/2	Not Critical
6. Plenum Chamber	Dissipative/ Suppressive	Broadband	D>1	D>1	Not Critical
7. Water Injection	Dissipative	Broadband	Unbounded		Not Critical

Table 1: Classification of Mufflers[12]

2.3.1 Helmholtz Principle

However in recent years an add-on solution using the Helmholtz concept has been developed in the form of Helmholtz Resonators. Helmholtz resonance is the phenomenon of air resonance in a cavity, when air is forced into a cavity, the pressure inside increases. When the external force pushing the air into the cavity is removed, the higher-pressure air inside will flow out. This surge of air flowing out tends to over-compensate, due to the inertia of the air in the neck, and the cavity will be left at a pressure slightly lower than the outside, causing air to be drawn back in. This process repeats with the magnitude of the pressure changes decreasing each time.

There exist many variations of the Helmholtz Resonators in the form of quarter-wavelength resonator [6], branched type resonator [5] and Duct resonators [1, 2]. Some of them are listed with some of their characteristics in Table 1 where f, c, λ are frequency, speed of sound, wavelength and the critical dimension respectively [9]. Theoretically D is unbounded but practically it has a bound which is D< ¼. The study here focuses on Lumped element model of Helmholtz Resonators.

2.3.2 Lumped element model of the Helmholtz resonator

The Helmholtz resonator is said to act as an acoustic filter element. If the dimensions of the Helmholtz resonator are smaller than the acoustic wavelength, then the dynamic behavior of the Helmholtz resonator can be modeled as a lumped system.

Essentially the system can be approximated as a mass-spring system and consequently it can be treated mathematically as such. The large volume of air is taken as a spring element and the air in the neck is considered as an oscillating mass. Damping appears in the form of radiation losses at the neck ends and viscous losses due to friction of the oscillating air in the neck. Fig. 1.3 shows this analogy between Helmholtz resonator and a vibration absorber.
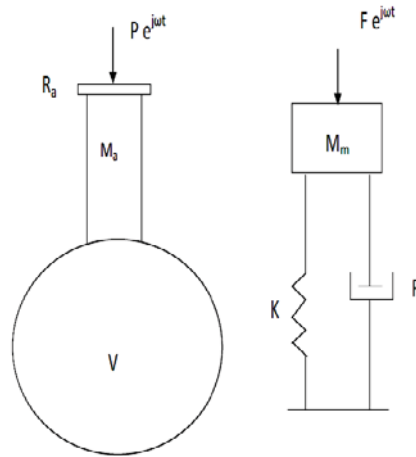
Figure 2.2 One Degree of Freedom Helmholtz resonator and vibration absorber

2.3.3 Analytical analysis of Single Helmholtz resonators

For a neck which is flanged at both ends [10], the effective length is approximately:

$$L_{eff} = L + 1.7a. \tag{2.2}$$

Which includes a correction factor for mass-loading due to air entrapment near the neck extremities, where 'a' is the radius of the neck .The acoustic mass of a Helmholtz resonator is given by

$$M_a = L_{eff}\rho S \tag{2.3}$$

Where S is the cross –sectional area of the neck, ρ is the density of the fluid. If 'y' denote the displacement of in the positive direction pointing inwards along the neck axis Fig. 1.3 then the stiffness of the resonator is defined as the reciprocal of the compliance, and it is defined as:

17

$$K_r = \frac{dF}{dy} \tag{2.4}$$

where

$$F = PS \tag{2.5}$$

Where 'F' is the force applied in the '+y' direction at the resonator neck entrance, P is the pressure at the neck entrance. For adiabatic system with air as an ideal gas, the thermodynamic process equation for the resonator is

$$PV^\gamma = C \tag{2.6}$$

Where C is a constant, Υ is the ratio of specific heats; V is the cavity volume of the resonator. Differentiating this equation gives

$$V^\gamma dP + P\gamma V^{\gamma-1} dV = 0 \tag{2.7}$$

Form Eqn. (2.5) the differential change in pressure dP is given by

$$dP = \frac{dF}{S} \tag{2.8}$$

The change in the cavity volume is

$$dV = -Sdy \tag{2.9}$$

which is negative since the air in the volume is compressed. Substituting these into differential equation, it can be re-casted as

18

$$V^{\gamma}\frac{dF}{S} - P\gamma V^{\gamma-1}Sdy = 0 \qquad (2.10)$$

This becomes,

$$\frac{dF}{dy} = \frac{p\gamma S^2}{V} = K_r \qquad (2.11)$$

or considering $P = \rho RT$ and $c = \sqrt{\gamma RT}$, resonator stiffness is then:

$$K_r = \frac{\rho c^2 S^2}{V} \qquad (2.12)$$

where c is the speed of sound.

Two sources of damping in the Helmholtz resonator can be considered: sound radiation from the neck and viscous losses in the neck, which in many cases can be neglected compared to radiation losses.

Sound radiation resistance is a function of the outside neck geometry. For a flanged pipe, the radiation resistance is theoretically determined and is approximately [10]

$$R_r = \frac{\rho c k^2 S^2}{2\pi} \qquad (2.13)$$

Where k is the wave number, $k = \dfrac{\omega}{c}$

On the other hand the mechanical resistance due to viscous losses can be considered as [11]

$$R_v = 2R_S S \frac{(L+a)}{\rho c a} \tag{2.14}$$

Where 'L' is the neck length, 'a' is the neck radius. R_s for a sufficiently large neck diameter is

$$R_S = 0.00083 \sqrt{\frac{\omega}{2\pi}} \tag{2.15}$$

where w is the excitation frequency.

The mechanical impedance of the mechanical system is defined as the ratio of the driving force and the velocity of the system at the driving point. The mechanical impedance of a driven mass-spring–damper system is [10]

$$\hat{Z}_m = \frac{\hat{F}}{\hat{u}} = R_m + j(\omega m - \frac{K_r}{\omega}) \tag{2.16}$$

Where R_m denotes viscous damping, 'm' is the mass element, and 'K_r' is the stiffness of the spring element. According to the analogy between Helmholtz resonator and mass-spring–damper system (vibration absorber), the mechanical impedance of a Helmholtz resonator is obtained by replacing mass and damping from Helmholtz resonator system in above equation:

$$\hat{Z}_{mres} = (R_v + \frac{\rho c k^2 S^2}{2\pi}) + j(\omega \rho L_{eff} S - \frac{\rho c^2 S^2}{\omega V}) \tag{2.17}$$

The natural frequency of a Helmholtz resonator "ω_0" is the frequency for which the reactance is zero:

20

$$\omega_0 = c\sqrt{\frac{S}{L_{eff}V}} \tag{2.18}$$

And the acoustic impedance of the side branch Helmholtz resonator is

$$\hat{Z}_{res} = \frac{\hat{Z}_{mres}}{S^2} \tag{2.19}$$

For an accurate prediction of the resonant frequency in one Degree of Freedom (DOF) cylindrical resonators the following Eqn. (2.20) can be used [8].

$$f = \frac{c}{2\pi}\sqrt{-\frac{3.L_n + L_c\lambda}{2L_n{}^3} + \sqrt{\left(\frac{3.L_n + L_c\lambda}{2L_n{}^3}\right)^2 + \frac{3\lambda}{L_n{}^3 L_c}}} \tag{2.20}$$

where λ is the ratio of area of cross section of the neck and the volume and L_c, L_n are the lengths of the cavity and the neck respectively. The only restriction in the above mentioned formulae is diameter must be less than a wavelength at the resonance frequency. The transmission loss (TL) for one DOF can also be calculated using the equation [7].

$$TL = 10Log_{10}\left[1 + \left(\frac{a_n}{2.a_d}\frac{(1/\lambda)\tan(k.L_c) + \tan(k.L_n)}{(1/\lambda)\tan(k.L_n)\tan(k.L_c) - 1}\right)^2\right] \tag{2.21}$$

Where k is the wave number and a_n and a_d are the area of cross section of the duct and neck respectively.

A formula for resonant frequencies was developed in the late nineteenth century which includes the effect of the geometry of the resonators [21].

$$f = \frac{c}{2\pi} X \sqrt{\frac{F_N}{1.21(V+V_N)\left\{\frac{V}{V+V_N+V_{O1}}-\frac{h}{h+l_N+l_{O1}}\left[l_v+(l_N+l_{O1})\left(1+\frac{1}{2}[\frac{V_N+V_{O1}}{V}+\frac{l_N+l_{O1}}{h}]+\frac{1}{3}\frac{V_N+V_{O1}}{V}-\frac{l_N+l_{O1}}{h}\right)+l_{O2}\right]\right\}}}$$ (2.22)

$$l_v = \frac{F_N}{Vh}\int_0^h \frac{xV(x)}{F(x)}dx$$ (2.23)

(here $F(x)$ is the area of a cross-section of the resonator expressed as a function of distance x from the bottom and

$$V(x) = \int_0^x F(\xi)d\xi$$ (2.24)

l_{O1}, l_{O2} = two parts of the total end-correction length due to the motion of gas particles outside the resonator .Generally the values $l_{O1} = l_{O2} = 0.24r$, where r is the radius of the neck or opening of the resonator.

V_{O1} = volume of the hypothetical elongation of the neck due to the motion of gas particles outside the resonator ($V_{O1} = F_N l_{O1}$).

2.3.4 Form factor (l_v) for fundamental forms of volumes in 1 DOF configuration

Form factor is calculated to calculate the effects of forms of volumes of the resonator. Following are the different form factors for volumes [21].

1. *Sphere.*
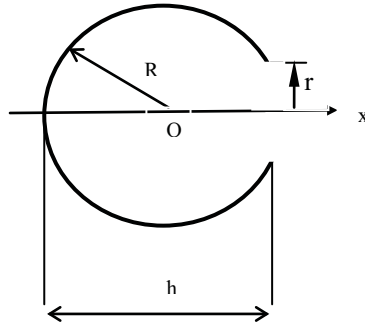
Figure 2.3 Spherical Helmholtz resonator

$$l_v = \frac{r^2}{R}\frac{1}{2-A}\left[\frac{1}{3} - \frac{1}{2(A+1)} - \frac{2}{(A+1)^2} + \frac{4}{(A+1)^3}\ln\frac{2}{1-A}\right] \tag{2.25}$$

Where, $A = \sqrt{1-(r/R)^2}$

2. *Frustum of a cone*
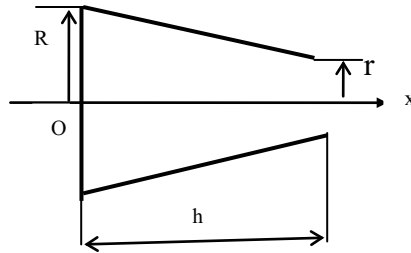
Figure 2.4 Conical Helmholtz resonator

$$l_v = \frac{h}{(R/r)^2 + (R/r) + 1}\left[\frac{1}{3} - \frac{R}{2(R-r)} - \left(\frac{R}{R-r}\right)^3\left(\frac{R}{r} - 1 - \ln\frac{R}{r}\right)\right] \tag{2.26}$$

23

3. Cylinder
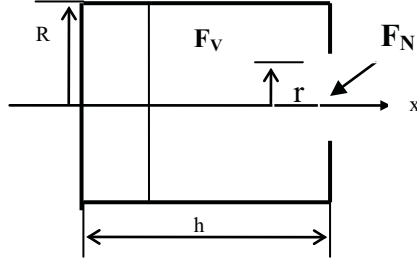
Figure 2.5Cylindrical Helmholtz resonator

$$l_v = \frac{F_N h}{3 F_V} \tag{2.27}$$

2.3.5 Analytical analysis of Two Degree of Freedom (Dual) Helmholtz resonators

In light of the low frequencies of interest in the present study, the geometrical dimensions considered here are significantly smaller than the relatively long wavelengths. Hence, the spatial resolution is ignored next to develop expressions for both the resonance frequencies and transmission loss for a dual Helmholtz resonator installed in a side branch orientation as shown in Fig. 2.6.

The resonance frequencies of Two DOF (Dual) Helmholtz resonators are calculated using the Eqn. (1.29)

$$f_{1,2} = \frac{c}{2\sqrt{2}\pi} \sqrt{\left(\frac{A_{C1}}{l'_{C1} V_1} + \frac{A_{C2}}{l'_{C2} V_1} + \frac{A_{C2}}{l'_{C2} V_2} \right) \pm \sqrt{\left(\frac{A_{C1}}{l'_{C1} V_1} + \frac{A_{C2}}{l'_{C2} V_1} + \frac{A_{C2}}{l'_{C2} V_2} \right)^2 - 4 \frac{A_{C1}}{l'_{C1} V_1} \frac{A_{C2}}{l'_{C2} V_2}}} \tag{2.28}$$

The Transmission loss of the Two DOF (Dual) Helmholtz resonator is then expressed as

$$TL = 20\log_{10}\left|1 + \frac{A_{C1}}{2A_P}\frac{1}{iKl'_{c1} + \frac{A_{C1}}{iKV_1}\left(1 - \frac{A_{C2}V_2}{A_{C2}V_2 + A_{C2}V_1 - V_2V_1K^2l'_{C2}}\right)}\right| \qquad (2.29)$$

The resonant frequencies for the different geometries with equal volume can be calculated by the formula

$$f_{1,2} = \frac{c\sqrt{A}}{2\pi\sqrt{2V}}f(l'_{c1},l'_{c2}) \qquad (2.30)$$

Where,

$$f(l'_{c1},l'_{c2}) = \left[\left(\frac{1}{l'_{c1}} + \frac{2}{l'_{c2}}\right) \pm \left[\left(\frac{1}{l'_{c1}} + \frac{2}{l'_{c2}}\right)^2 - \frac{4}{l'_{c1}.l'_{c2}}\right]^{\frac{1}{2}}\right]^{\frac{1}{2}} \qquad (2.31)$$

In order to combine the effects of end correction factors [10], Eqns. (2.35) and (2.36) can be considered.

An end correction that accounts for the higher order wave propagation between the neck and the cavity is given by Eqn. (2.35) and the higher order wave propagation effects between the circular neck and main pipe, the end correction is approximated by Eqn. (2.36). [11]

25
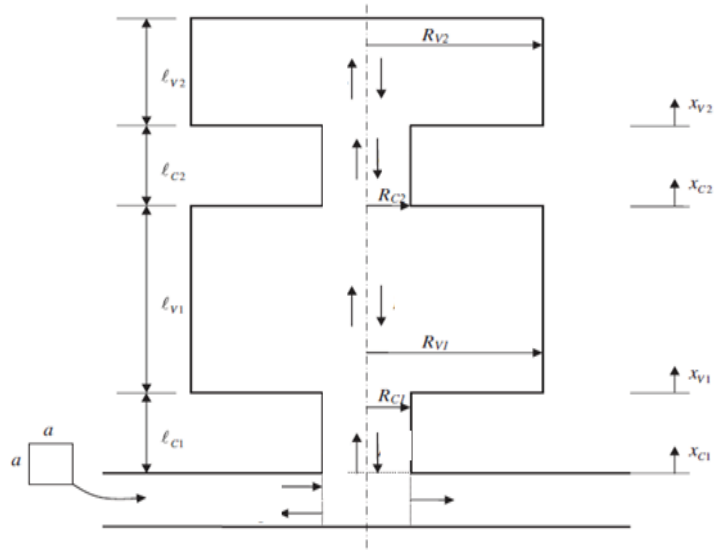
Figure 2.6 Schematic display of a branched 2DOF(Dual) Helmholtz Resonator [8]

A= Area of cross-section of the neck

V=Volume of the resonator

c=Speed of sound

$l_{c1}{}'$=Corrected length of the neck of the first geometry

$l_{c2}{}'$=Corrected length of the neck of the second geometry

$$l'_{c1} = l_{c1} + \delta_v + \delta_p \qquad (2.32)$$

$$l'_{c2} = l_{c2} + 2\delta_v \qquad (2.33)$$

$$\delta_v = 0.85R_{neck}\left(1 - 1.25\frac{R_{neck}}{R_{volume}}\right) \tag{2.34}$$

$$\delta_p = 0.82\frac{R_{neck}}{2} \tag{2.35}$$

The classic lumped approach approximates this resonator as an equivalent spring (cavity) and mass (neck) system, and yields the expressions for the resonator frequency and the transmission loss [11,12], [19-21]. A number of studies [13,15], [22-24]have also developed a one-dimensional analytical approach to investigate the wave attenuation properties. To account for the non-planar wave propagation in both the neck and the cavity, multi-dimensional analytical approaches have also been employed to predict the sound attenuation in Helmholtz resonators with circular concentric cavity [24], circular asymmetric cavity [25], extended neck [26], and lined with absorbing material. To improve the sound attenuation performance, Helmholtz resonators with a variety of modifications have been examined. Selamet and Lee [26] studied the effect of length, shape, and perforation of the neck extension on the resonance frequency and transmission loss of concentric circular Helmholtz resonators with extended neck. Selamet et al. [27] developed a closed-form, 2D analytical solution to investigate the effect of density and thickness of the fibrous material in the cavity on the resonance frequency and transmission loss of circular Helmholtz resonators lined with absorbent. Tang [28] experimentally and theoretically investigated the Helmholtz resonators with tapered necks with the cross-sectional area increasing towards cavity. Griffin et al. [29]

developed an analytical model for a single, coupled resonator system mounted on a one-dimensional duct. The proposed mechanically-coupled resonators produced a particular transmission loss response, provided a wider bandwidth of attenuation, and adapted the transmission loss characteristics of a structure to attenuate disturbances of varying frequency. Wan and Soedel [30] derived an expression for the resonance frequencies of 2- DOF Helmholtz resonator using a lumped analysis. They obtained the resonance frequencies and compared them to the computational results and measurements. De Bedout et al. [31] proposed a tunable Helmholtz resonator with a feedback.

2.4 PROBLEM STATEMENT

Currently Dresser-Rand uses Duct Resonator arrays (DR arrays) as an add-on solution [1, 2]. The solution was applied successfully to a 2528 PSIG (172 BARG) multistage centrifugal compressor on a platform in the North Sea and was shown to successfully give a reduction of up to 12 dBA. Over the last few years, Dresser Rand has revamped more than 61 centrifugal compressors, both single stage and multistage [1, 2], with the DR arrays. Although the Dresser Rand arrays give appreciable noise reduction, our work is focused on how to reduce noise coming out of the compressor and transmitted into the pipelines. Keeping in mind the research done in this field, the current scenario calls for a design methodology which can be used for designing the one and two degree of freedom resonators for maximum noise reduction. No such effort has been made so far and that will somehow aid the industrial engineers to design such a thing with minimal efforts from research point of view. Another important thing is the response

of different geometrical configurations on the noise reduction process which also demands attention. The method of noise reduction using Helmholtz resonator has to be investigated thoroughly to search for a possible solution for noise transmitted in the pipelines.

2.5 CONCLUSION

A thorough literature review has been done on sources of noise generation in compressors and the various techniques developed so far for its attenuation. Helmholtz resonators principle is described in detail with analysis of both one and two degree of freedom Helmholtz resonators. Our focus in this study is lumped element model of the Helmholtz resonator. Various researches done in this field of Helmholtz resonators and other ways of noise reduction is also covered in this chapter. The problem statement is defined and a solution has been proposed in the upcoming chapters. The accuracy of the proposed solutions were validated using finite element method and with experimental results in some cases.

CHAPTER 3

ANALYTICAL DERIVATION OF TRANSMISSION

LOSS OF ONE AND TWO DEGREE OF FREEDOM

RESONATORS

Transfer matrix or Four-Pole parameter method is used for the derivation of Transmission Loss of the Resonators. According to this method all the elements of the acoustics filter can be written in the form of elements of transfer matrix.

3.1 ONE DEGREE OF FREEDOM

Adopting acoustic Pressure p and mass velocity v as the two state variables, the following matrix relation can be written so as to relate state variables [12],[16].

$$
\begin{bmatrix} p_m \\ v_m \end{bmatrix} = \begin{bmatrix} A\ 2\text{X}2\ matrix \\ for\ the\ m^{th} \\ element \end{bmatrix} \begin{bmatrix} p_{m-1} \\ v_{m-1} \end{bmatrix} \tag{3.1}
$$

on the two sides of the element . $[p_m, v_m]$ is called the state vector at the upstream point m and $[p_{m-1}, v_{m-1}]$ called the state vector at the downstream point m-1 [17]. The transfer matrix for the m*th* element can be denoted by $[T_m]$ which is,[35]

$$[T_m] = \begin{bmatrix} \begin{pmatrix} A_{11} & A_{12} \\ A_{21} & A_{22} \end{pmatrix} \end{bmatrix} \tag{3.2}$$

On making use of standing wave relation Munjal(1987) derived the four parameters which resulted in closed form relationship[12],

$$\begin{bmatrix} p_m \\ v_m \end{bmatrix} = \begin{bmatrix} \begin{pmatrix} Cos(k_o l_m) & jY_m Sin(k_o l_m) \\ j/Y_m Sin(k_o l_m) & Cos(k_o l_m) \end{pmatrix} \end{bmatrix} \begin{bmatrix} p_{m-1} \\ v_{m-1} \end{bmatrix} \tag{3.3}$$

Where, Y_m is the characteristic impedance, k is the wave number, j is the imaginary number and l_m is the effective length of the element.

On applying the continuity condition for velocity and pressure Fig 3.1,

$$V_i(x) = V_t(x) + V_r(x) \tag{3.4}$$

$$P_i(x) = P_t(x) = P_r(x) \tag{3.5}$$

In matrix form, Eqns. (3.4) and (3.5) can be written as[33]

$$\begin{bmatrix} P_i \\ V_i \end{bmatrix} = \begin{bmatrix} 1 & 0 \\ V_r/P_t & 1 \end{bmatrix} \begin{bmatrix} P_t \\ V_t \end{bmatrix} \tag{3.6}$$
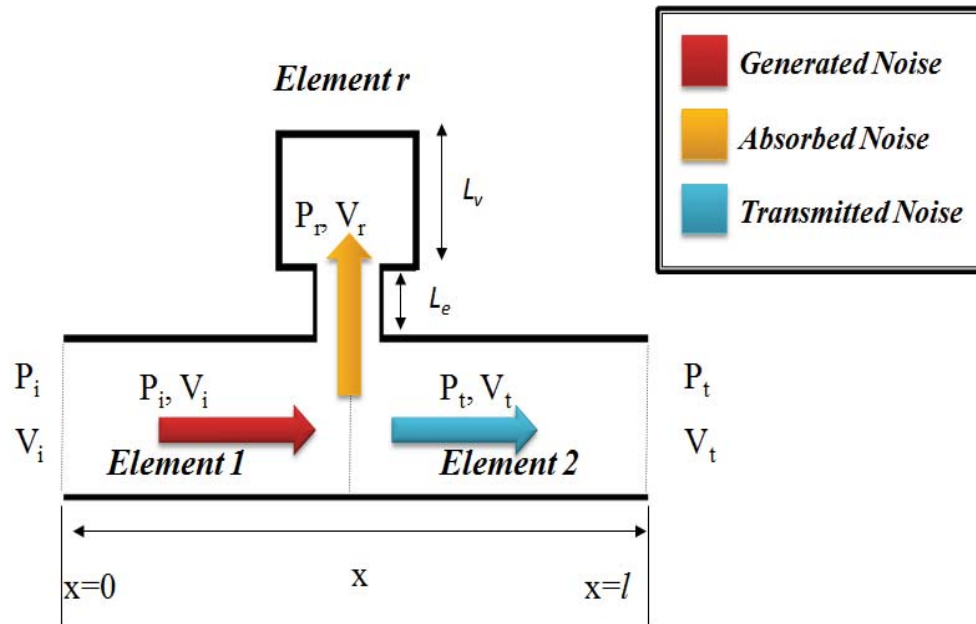
Figure 3.1 A one degree of freedom Helmholtz resonator attached to a circular duct

Since,

$$P_t(x) = P_r(x) \tag{3.7}$$

And

$$Z_r = V_r / P_r \tag{3.8}$$

Eqn. (3.6) can be written as

$$\begin{bmatrix} P_i \\ V_i \end{bmatrix} = \begin{bmatrix} 1 & 0 \\ 1/Z_r & 1 \end{bmatrix} \begin{bmatrix} P_t \\ V_t \end{bmatrix} \tag{3.9}$$

Where the matrix $\begin{bmatrix} 1 & 0 \\ 1/Z_r & 1 \end{bmatrix}$ represents the transfer matrix of the Helmholtz

Resonator. Z_r is the impedance at the opening of the attached Helmholtz Resonator, which can be calculated by following the same method as discussed. Taking area of cross section of the neck as 'a', area of cross section of the volume as, 'a_v', length of the neck as 'L_e', length of the volume as 'L_v', the input impedance of the resonator comes out to be,

$$Z_r = \frac{Cos(kL_e)Cos(kL_v) - (a_v/a)Sin(kL_e)Sin(kL_v)}{i(a/c)Cos(kL_v)Sin(kL_e) - i(a_v/c)Cos(kL_e)Sin(kL_v)} \tag{3.10}$$

The complete transfer matrix of the duct HR system shown in Fig.(3.1) can be represented by the equation

$$\begin{bmatrix} P_i \\ V_i \end{bmatrix} = \begin{bmatrix} A\,2X2\,matrix \\ of\,the\,element\,1 \end{bmatrix} \begin{bmatrix} A\,2X2\,matrix \\ of\,the\,element\,r \end{bmatrix} \begin{bmatrix} A\,2X2\,matrix \\ of\,the\,element\,2 \end{bmatrix} \begin{bmatrix} P_t \\ V_t \end{bmatrix} \tag{3.11}$$

Where the four poles for any element m with length 'l_m', and characteristic impedance 'Z_m'is given by[12]

$$\begin{aligned} A_{11} &= Cos(k_o l_m) \\ A_{12} &= jZ_m Sin(k_o l_m) \\ A_{21} &= j/Z_m Sin(k_o l_m) \\ A_{22} &= Cos(k_o l_m) \end{aligned} \tag{3.12}$$

On taking 'a_d' as the duct cross section area and solving we derive the equation in the form,

$$\begin{bmatrix} P_t \\ V_t \end{bmatrix} = \begin{pmatrix} T_{11} & T_{12} \\ T_{21} & T_{22} \end{pmatrix} \begin{bmatrix} P_i \\ V_i \end{bmatrix} \qquad (3.13)$$

Now the four parameters in the final transfer matrix can be used to calculate the transmission loss of the Helmholtz resonator. According to Munjal (1987), the transmission loss for the equation [12]

$$\begin{bmatrix} P_n \\ V_n \end{bmatrix} = \begin{pmatrix} T_{11} & T_{12} \\ T_{21} & T_{22} \end{pmatrix} \begin{bmatrix} P_1 \\ V_1 \end{bmatrix} \qquad (3.14)$$

is given by Eqn. (2.15)

$$TL = 20 Log_{10} \left[\left(\frac{Z_1}{Z_n} \right)^{0.5} \left| \frac{T_{11} + (T_{12}/Z_1) + Z_n.T_{21} + (Z_n/Z_1)T_{22})}{2} \right| \right] \qquad (3.15)$$

On calculating the TL from the equation mentioned above, it comes out to be

$$TL = 10 Log_{10} [1 + \frac{2a^2(a_v^2 + a^2 + (a^2 - a_v)Cos(2kL_c))}{4\, a_d^2.(2aCos(kL_c)Cos(kL_e) - 2a_v Sin(kL_c)Sin(kL_e))^2} \\ - \frac{a^2}{4.a_d^2}] \qquad (3.16)$$

The TL for 'n' resonators can also be calculated using the same procedure, but in that case the final transfer matrix will have the form,

$$\begin{bmatrix} P_i \\ V_i \end{bmatrix} = \begin{bmatrix} A\,2X2\,matrix \\ of\,the\,element\,1 \end{bmatrix} \begin{bmatrix} A\,2X2\,matrix \\ of\,the\,element\,r \end{bmatrix} \begin{bmatrix} A\,2X2\,matrix \\ of\,the\,element\,n-1 \end{bmatrix} \begin{bmatrix} P_t \\ V_t \end{bmatrix} \qquad (3.17)$$

34

3.2 TWO DEGREE OF FREEDOM

The above mentioned procedure can be used again for formulation of TL equation of two degree of freedom resonators (neck–cavity–neck– cavity).On evaluating the Transmission loss the result has similar solutions as obtained from the published equation Eq. (3.18) where the values can be correlated with Fig. 1.7 [10]

$$TL = 20\log_{10}\left|1+\frac{A_{C1}}{2A_P}\cfrac{1}{iKl'_{c1}+\cfrac{A_{C1}}{iKV_1}\left(1-\cfrac{A_{C2}V_2}{A_{C2}V_2+A_{C2}V_1-V_2V_1K^2l'_{c2}}\right)}\right| \tag{3.18}$$

CHAPTER 4

DESIGN PROCEDURE FOR ONE AND TWO DOF

RESONATORS

4.1 DESIGN OF 1-DOF RESONATORS

It is known from Selamet [8] and [10] that resonating frequency and transmission loss for one DOF Helmholtz resonator are represented by Eqn.(4.3) & (4.4). The design parameters are four: L_c, L_n, a_c, a_n. Relationships need to be defined to proceed with suitable design. The design procedure to estimate optimal size for the resonator needs to satisfy a couple of conditions derived from the frequency equation and the transmission loss equation. We call the initial condition as a necessary condition which relates the parameters and is given here.

$$f < 0.2756 \frac{c}{L_c} \tag{4.1}$$

The second equation is the **necessary condition** derived from the optimum transmission loss [8]

$$\lambda = \frac{a_n}{a_c} = \tan(k\,L_n).\tan(k\,L_c) \tag{4.2}$$

The resonant frequency for 1 DOF resonators can be calculated using the formula[8]

$$f = \frac{c}{2\pi}\sqrt{-\frac{3.L_n + L_c\lambda}{2L_n^{\,3}} + \sqrt{\left(\frac{3.L_n + L_c\lambda}{2L_n^{\,3}}\right)^2 + \frac{3\lambda}{L_n^{\,3}L_c}}} \tag{4.3}$$

The only restriction in the above mentioned formulae is that cavity diameter must be less than a wavelength at the resonance frequency. And the Transmission loss can be calculated using [10]

$$TL = 10Log_{10}\left[1+\left(\frac{a_n}{2.a_d}\frac{(1/\lambda)\tan(k.L_c)+\tan(k.L_n)}{(1/\lambda)\tan(k.L_n)\tan(k.L_c)-1}\right)^2\right] \tag{4.4}$$

Where,

$$k = \frac{2\pi f}{c}$$

$l_c = 6.2$ mm

$l_n = 2.5$ mm

$a_c = 32.17$ mm^2

$a_n = 19.63$ mm^2

$a_d = 1963.5$ mm^2
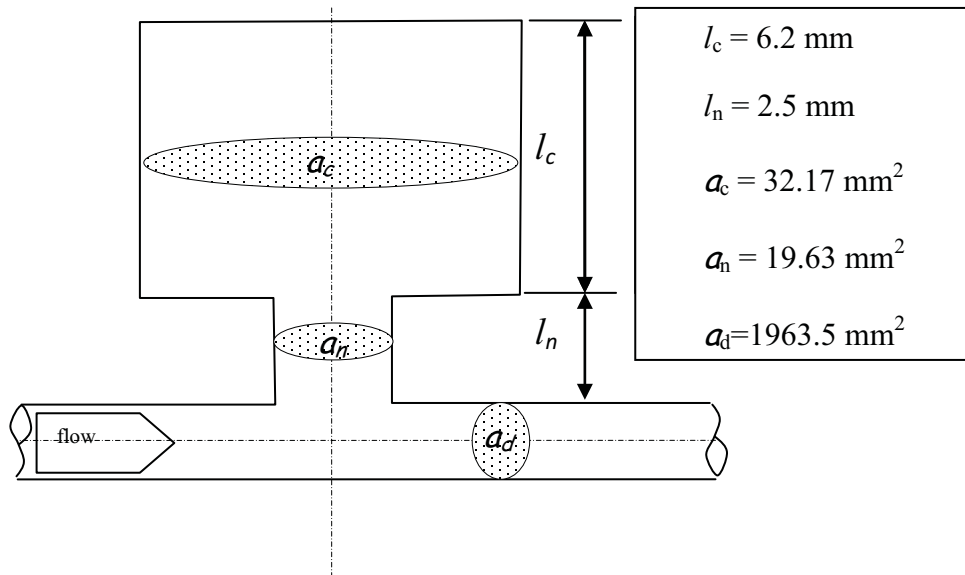
Figure 4.1Simple One DOF Helmholtz Resonator

A one degree of freedom Helmholtz resonator Fig (4.1) was designed using the design procedure and the values from published papers [10] were used to test the accuracy of the design. The values of the parameters are also mentioned in Fig (4.1).

Procedure:

- Assume values for λ in the range of 0 to 1.

- Approximate the maximum value of L_c from Eqn.(4.1)

- Calculate the values of L_n from the Eqn.(4.2)

- In order to combine the effects of end correction factors [10] the following equations are considered

$$l_n = L_n - \delta_1 - \delta_2$$

<div align="right">(4.5)</div>

- Assuming a value for an allowable radius of the neck calculate a_n and using that an end correction that accounts for the higher order wave propagation is[11]

$$\delta_2 = 0.48\sqrt{a_n}\left(1 - 1.25\sqrt{\lambda}\right)$$

<div align="right">(4.6)</div>

- To account for the higher order wave propagation effects between the circular neck and main pipe (one direction being infinite, while the size of the other direction is close to that of the neck), the end correction is approximated by

$$\delta_1 = 0.46\frac{\sqrt{a_n}}{2}$$

<div align="right">(4.7)</div>

- Define a minimal value for Δ through which we calculate a set of values of L_n by applying the equation $L_c = L_c - \Delta$.
- To close the choice of dimensions, the set of values giving the maximum value for transmission loss Eqn. (4.4) are the most suitable design parameters.

4.2 DESIGN OF A TWO DEGREE OF FREEDOM RESONATOR

$l_{n1} = 8.5$ cm

$a_{n1} = 12.57$ cm^2

$l_{n2} = 7.62$ cm

$a_{n2} = 9.62$ cm^2

$V_1 = a_{c1} . l_{c1} = 3706$ cm^3

$V_2 = a_{c2} . l_{c2} = 1853$ cm^3

$a_d = 18.48$ cm^2
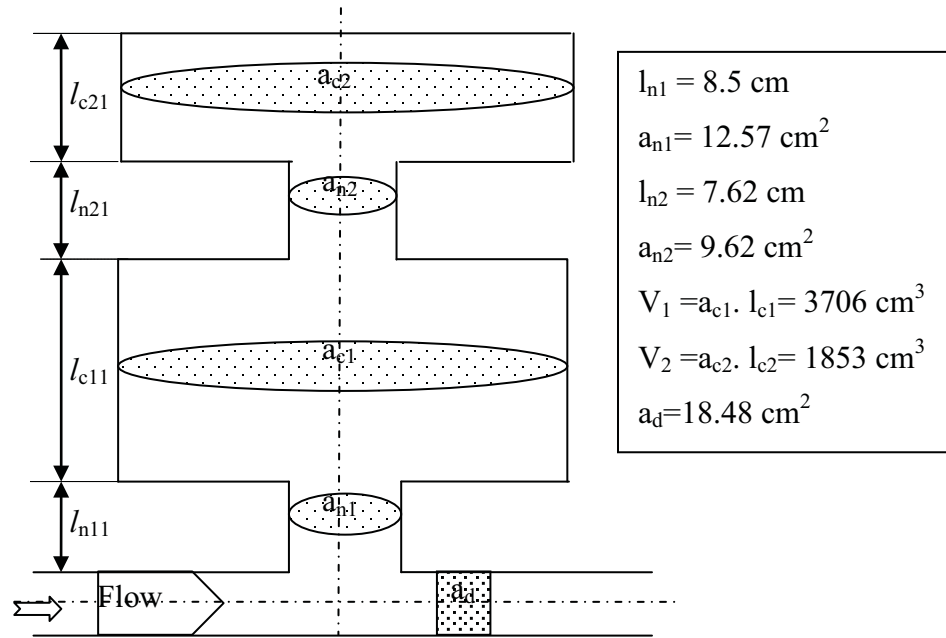
Figure 4.2 Dual Helmholtz Resonator [11]

Procedure:

Let the frequency to be attenuated as $f_{1,2}$

- Following the procedure for two DOF resonators calculate the values of the radius, neck length and the volume of the first resonator i.e. R_{n1} , l_{n1} ,V_1 . Calculate the ratio (γ_a /γ_l) which satisfies the **necessary condition** derived from (Eqn. A5**)** (See Appendix)

$$\frac{f_1^2}{f_2^2} + \frac{f_2^2}{f_1^2} \geq 2\left(1 + \frac{2\gamma_a}{\gamma_l}\right)$$

(4.8)

where

40

$$\gamma_a = \frac{a_{n2}}{a_{n1}}$$

$$\gamma_l = \frac{l_{n2}}{l_{n1}}$$

and a_{n1}, a_{n2} are the area of cross sections of the first and the second neck.

- Let $\alpha = \frac{a_{n1}}{l_{n1}}$ and $\beta = \frac{a_{n2}}{l_{n2}}$

$\frac{\gamma_a}{\gamma_l}$ can be determined from Eq.(4.1) and since it is equal to $\frac{\beta}{\alpha}$, this ratio can also be

calculated accordingly

- By using the below mentioned frequency equation, V_1 and V_2 can be calculated in terms of α and β.

$$f_{1,2} = \frac{c}{2\sqrt{2}\pi}\sqrt{\left(\frac{\alpha}{V_1}+\frac{\beta}{V_1}+\frac{\beta}{V_2}\right)\pm\sqrt{\left(\frac{\alpha}{V_1}+\frac{\beta}{V_1}+\frac{\beta}{V_2}\right)^2-4\frac{\alpha}{V_1}\frac{\beta}{V_2}}} \qquad (4.9)$$

Now the transmission loss can be calculate using Eqn. (4.3) but rewritten and plotted

w.r.t α and β, for getting the optimum $\frac{\beta}{\alpha}$ for maximum transmission loss. The corrected

lengths can be converted to original lengths used for design by following step (vi) of the

one degree of freedom design procedure.

$$TL = 20\log_{10}\left|1+\alpha \middle/ \left[2a_d\left(ik+\frac{\alpha}{ikV_1}\left(1-\frac{V_2}{V_2+V_1-\dfrac{V_2V_1k^2}{\beta}}\right)\right)\right]\right| \qquad (4.10)$$

where , a_d is the cross section area and k is the wave number.

This method has been applied to design a two DOF resonator for a pipeline. Referring to Fig. 4.2, the values can be correlated. The corresponding volume of the first and second cavities we simulated as being $V_1 = 3706$ cm^3 and $V_2 = 1853$cm^3 respectively. Fig. 4.2 and Fig. 4.3 shows the transmission loss distribution depending on the dimensional parameters ratios α and β. An in-depth analysis of the level of transmission loss that could be achieved shows that optimization can be done based on the acceptable manufactured necks in terms of diameters and lengths. As an estimation, 15-20 % away from the maximum transmission loss leads to a manufacturable shape of the resonator's neck.

4.3 SIMULATION RESULTS FOR ONE AND TWO DOF RESONATORS

4.3.1 Simulation for one degree of freedom resonator.

The following example is applied to an industrial plant. A cylindrical Helmholtz resonator was designed using the design procedure for one degree of freedom discussed earlier. The blade passing frequency that was attenuated was measured at the suction pipe of a compressor situated at Shedgum plant of Saudi Aramco Fig. (4.5). The simulation is shown in Fig. (4.7), where the pipe with the array of resonators is able to attenuate the noise by about 30 dB max.

The dimensions that were taken to model the resonators were found for $\lambda=0.1$ which are $r_{neck=}$ 1 mm, $l_{neck}=3.74$ mm, $r_{volume}=3.16$ mm, $l_{volume}=6.21$ mm. On comparing the pipe with the resonator array with the pipe without the arrays a sudden decrease in the sound pressure levels can be visualized Fig. 4.7. The pipe shown in fig 4.7 is able to attenuate noise by approximately 25-30 dB which can be considered an efficient design of the resonators. The transmission loss offered by the resonators can also be visualized by the peak of the curve at the designed frequency Fig 4.6.
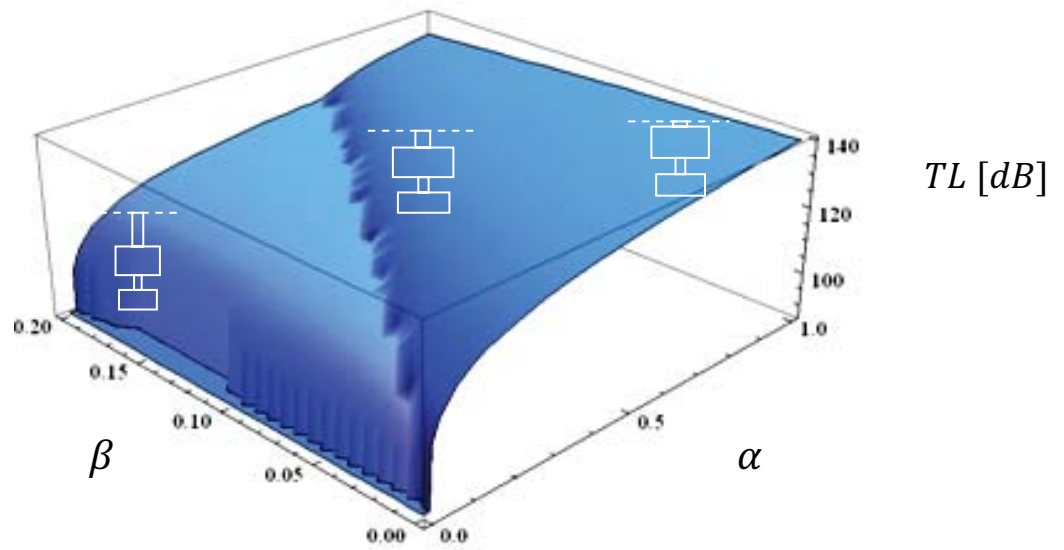
Figure 4.3 A 3D plot showing the variation of Transmission loss with respect to α and β for dual Helmholtz Resonator resonating at 5000 Hz.
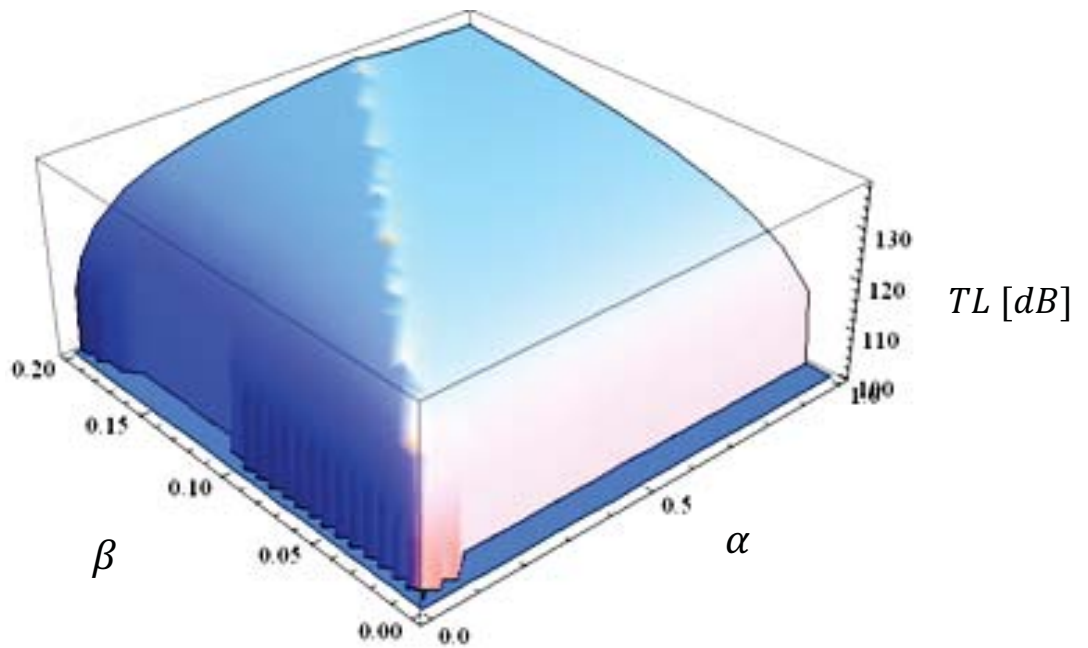

Figure 4.4A 3D plot showing the variation of Transmission loss with respect to α and β for dual Helmholtz Resonator resonating at 3000 Hz.

When more identical resonators are added on the same location around the perimeter of the pipe (Fig.4.9) it was observed that the sound pressure attenuation has improved by about 5%. This shows the advantage of using an array of resonators rather than a single resonator however the attenuation offered by the array has a very limited incremental range as shown in Fig.4.11. When comparing the results for the two configurations of arrays, i.e. one and four sets of resonators, the frequency for which they are designed doesn't match accurately showing a little difference of around 30-50 Hz Fig 4.11 It also shows the comparison of the degree of attenuation obtained between one and four sets of resonators. This happens because when array of resonators are put around their resonating frequencies some of them resonate for a particular value while others couldn't achieve full resonance for that value and this happens due to different orientations of the resonators and their slight misplacement around the sound carrying duct. This phenomenon can be perceived from Fig. 4.12 or for a closer look Fig. 4.13 can be viewed, where different SPL are encountered for a particular designed frequency in the resonators.

Another notable feature is that when using one resonator the reduction of noise takes a while Fig. 4.8, while in the case of four resonators the reduction is almost instant Fig. 4.10.This is evident from the sudden change in the contour colors which represents the sound pressure levels for each figure. The pattern followed by the sound waves inside the transmission duct is due to the small dimensions taken for the transmission duct Fig. 4.8. Also since plane wave assumption is taken in the simulations, the travelling waves gets reflected from the region where the resonator is fitted due to impedance mismatch, hence,

regions with varying sound pressure levels are encountered before the resonator Fig. 4.8. In the case of one resonator the crest of the waveform is unable to reach the resonator and therefore maximum possible reduction is not achieved Fig. 4.8, while in the case of four resonators the crest of the transmitted waves impinges exactly on the resonator neck and thereby due to resonance the reduction in noise achieved is of higher order Fig. 4.10.

The resonance mentioned above can be visualized by the sky blue circles formed around the necks of the resonators Fig. 4.10. In comparison to these circles the pipe fitted with just one resonator doesn't have any such phenomenon happening inside due to the reason already mentioned.
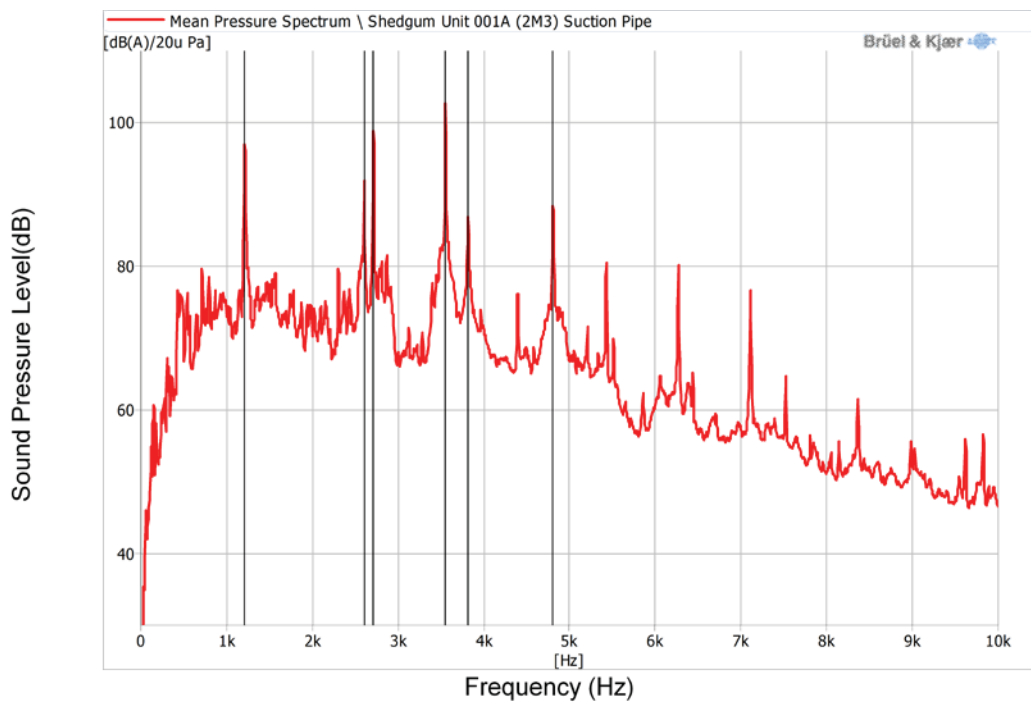
Figure 4.5 Suction Pipe Narrowband Sound Pressure Level of a measured compressor (DR).
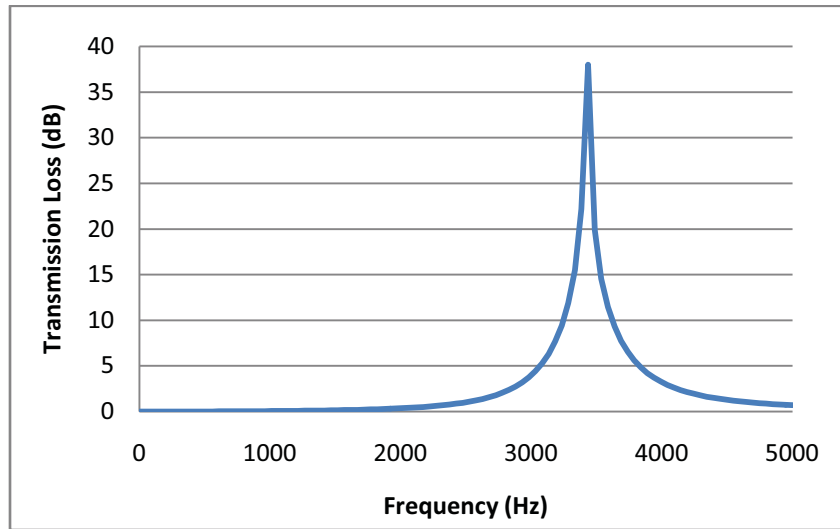
Figure 4.6 Sound Pressure levels at the another extreme of the pipe with and without the designed

resonators.
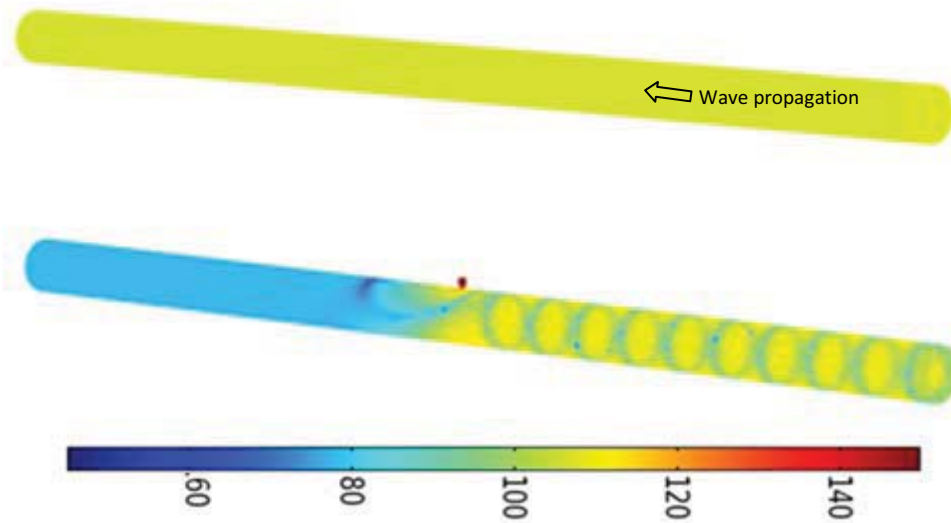
Figure 4.7 Sound Pressure levels distribution at 3556 Hz on the surface of the pipe with and

without 1 DOF designed resonators.

Surface: Sound pressure level

Wave propagation
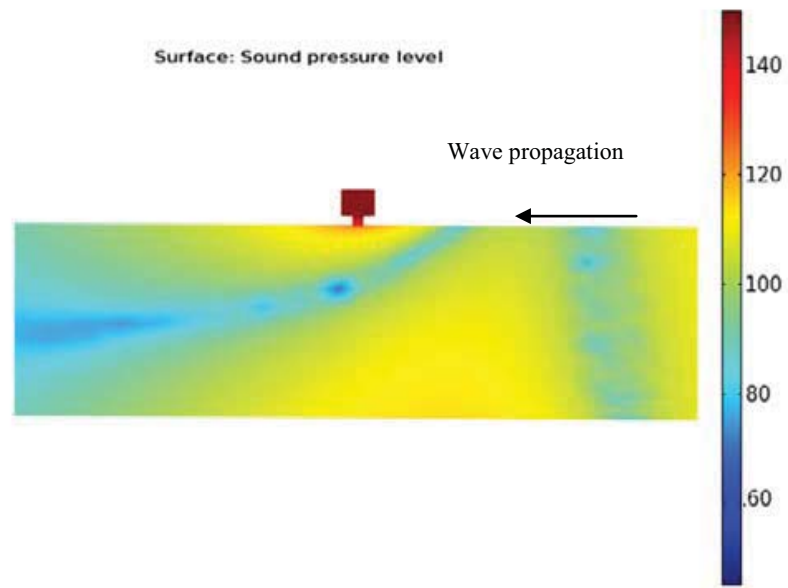
Figure 4.8 A closer view of the tuned resonator at 3556 Hz

Wave propagation
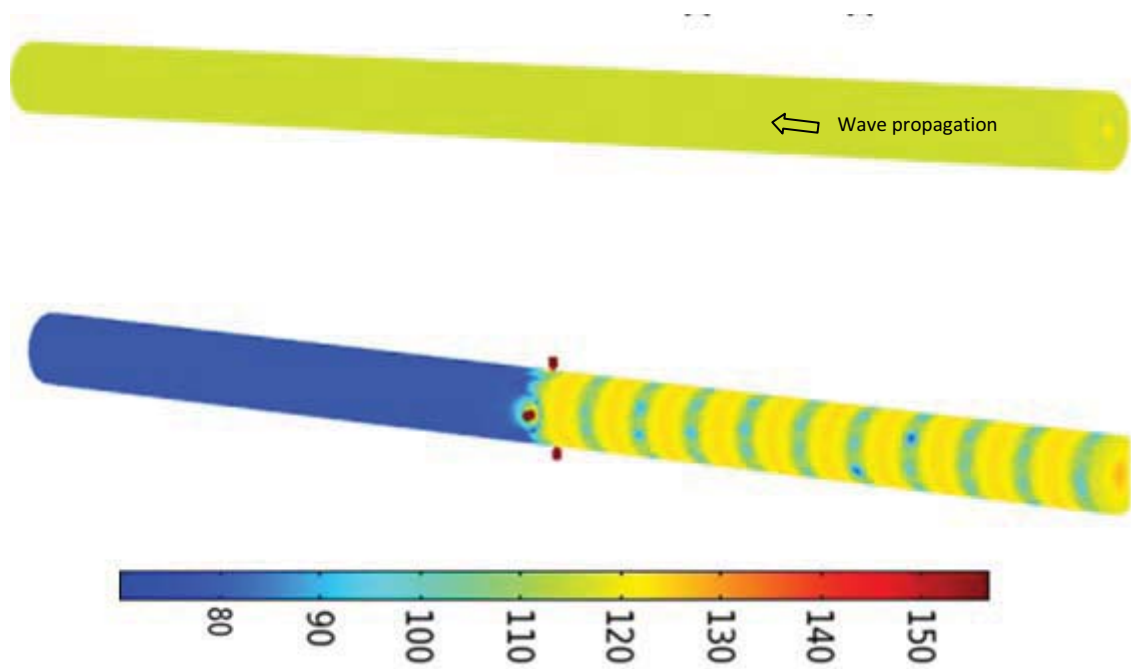
Figure 4.9: SPL distribution at 3556 Hz on the surface of the pipe with and without an array of

one DOF designed resonators.

Wave propagation
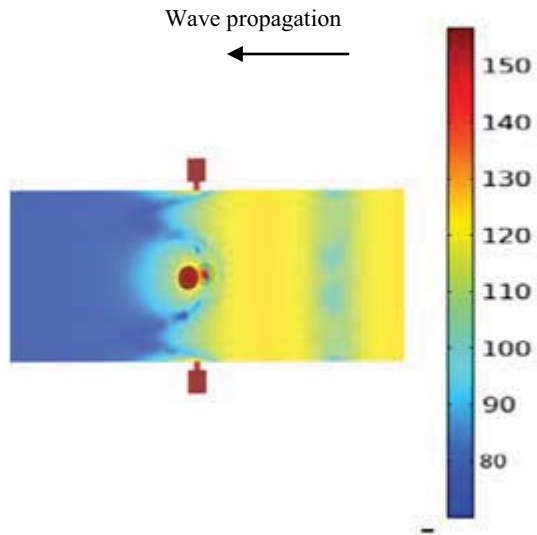
Figure 4.10 A closer view of the tuned resonator at 3556 Hz
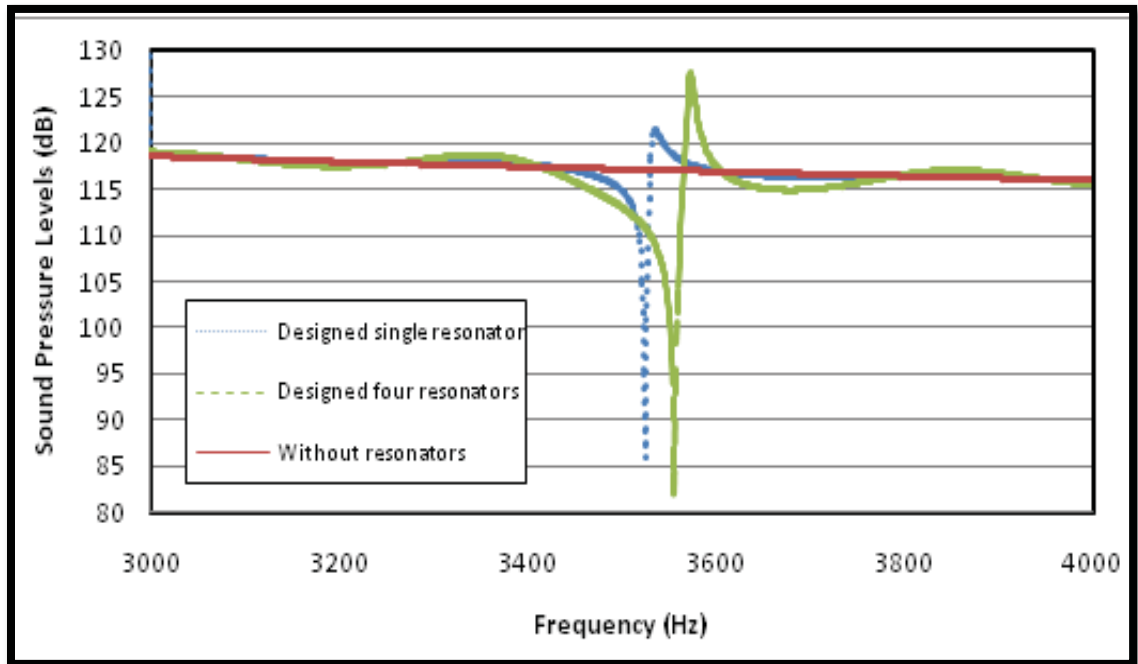
Figure 4.11 Comparison of Sound Pressure levels at the another extreme of the pipe with one

and four one DOF designed resonators.

4.3.2 Simulation for two degrees of freedom resonator

A 2 DOF cylindrical Helmholtz resonator was designed using the design procedure. This time two highest peaks from Fig. 4.5 were taken to be attenuated by designing resonators. The simulation shown in Fig. 4.12 and Fig. 4.15 gives an idea of the degree of attenuation received where the pipes with the array of resonators is able to attenuate the noise by around 30-40 dB for both frequencies. Fig. 4.12 shows the performance of the designed resonator for 3556 Hz while Fig. 4.14 shows the performance of the designed resonators for the other peak of 2712 Hz. Fig. 4.13 and Fig. 4.14 shows a closer view of the phenomenon taking place inside the resonators. The values of α and β taken are 1.2 and 0.07142 so as to satisfy Eqn. (4.1) i.e. the ratio $\frac{\beta}{\alpha} \leq 0.07522$, for frequencies 3556 and 2712 Hz.

The pattern followed by the sound waves inside the transmission duct is due to the small dimensions taken for the transmission duct Fig. 4.13 and Fig. 4.15. Again, since plane wave assumption is taken in the simulations, the travelling waves gets reflected from the region where the resonator is fitted due to impedance mismatch, hence, regions with varying sound pressure levels are encountered before the resonator Fig. 4.13. In the case of resonator tuned to 3556 Hz the crest of the waveform is unable to reach the resonator and therefore maximum possible reduction is not achieved Fig. 4.13, while in the case of resonators tuned to 2712 Hz the crest of the transmitted waves impinges

exactly on the resonator neck and thereby due to resonance the reduction in noise achieved is of higher order Fig. 4.15.

The resonance mentioned above can be visualized by the sky blue circles formed around the necks of the resonators Fig. 4.15. In comparison to these circles the pipe fitted with resonator tuned to 3556 Hz doesn't have any such phenomenon happening inside due to the reason already mentioned. Another notable feature, which can be visualized from Fig. 4.13, is the variation of sound pressure levels inside the two DOF resonators. The sound pressure levels of the two chambers of a two DOF resonators depends on the amount of noise absorbed by the respective chambers, i.e. the chamber which is tuned to the frequency will absorb more amount of noise and will thereby exhibit higher sound pressure levels and vice versa .
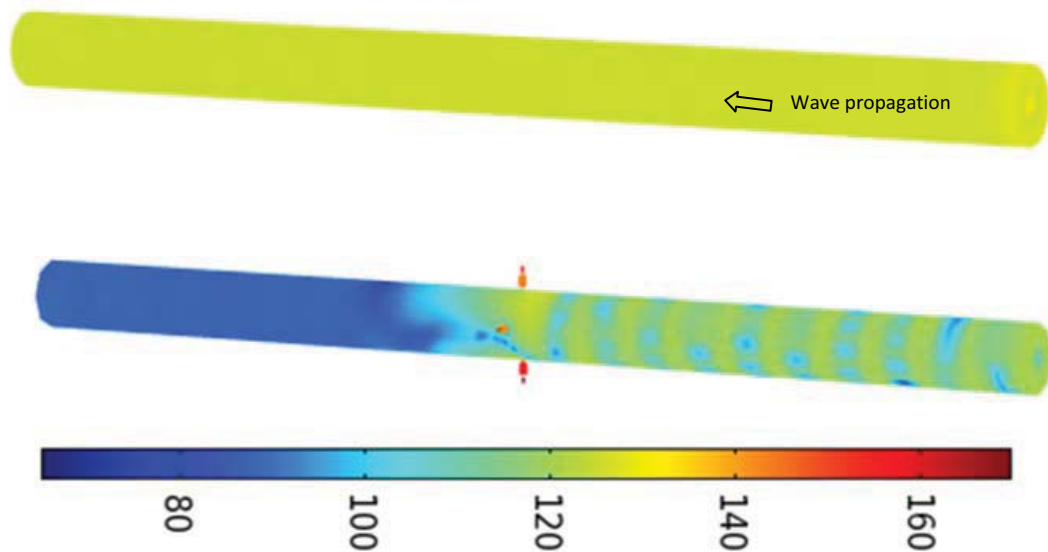
Figure 4.12 Sound Pressure levels distribution at 3556 Hz on the surface of the pipe with and without 2 DOF designed resonators.

51
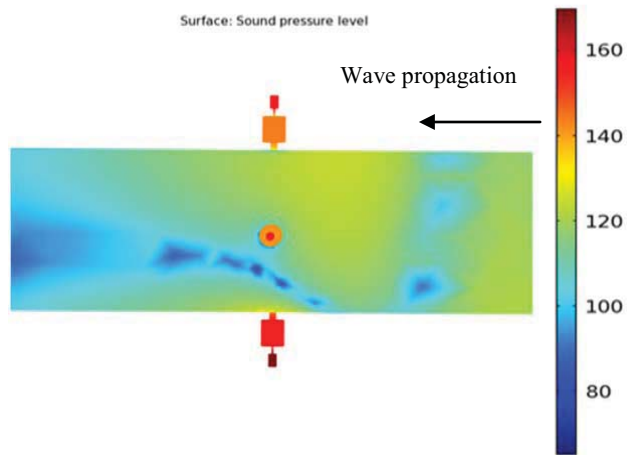
Figure 4.13 A closer view of Sound Pressure levels distribution at 3556 Hz on the surface of the

pipe with and without 2 DOF designed resonators.
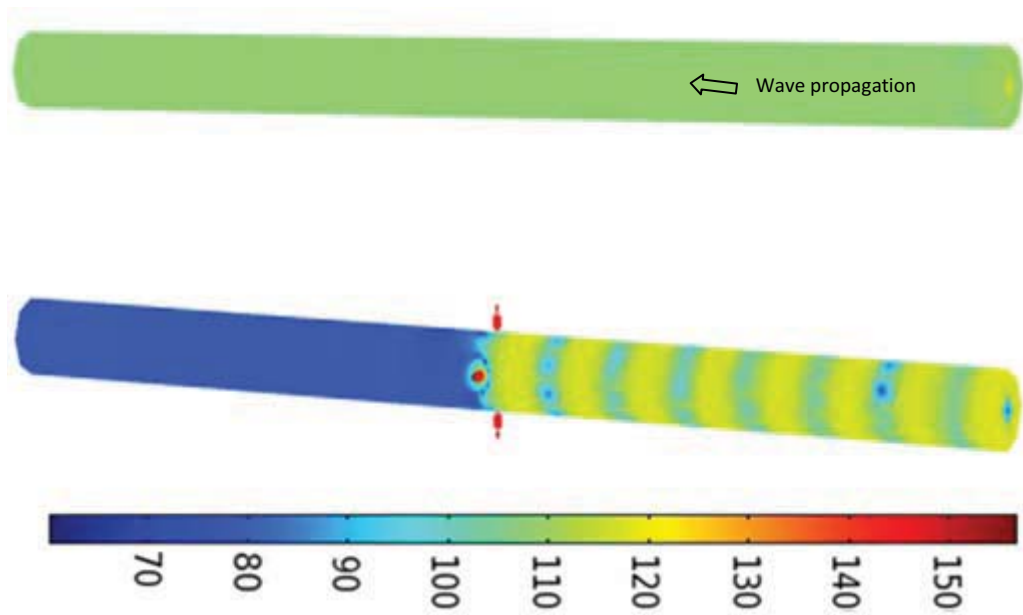
Figure 4.14 Sound Pressure levels distribution at 2712 Hz on the surface of the pipe with and

without 2 DOF designed resonators.
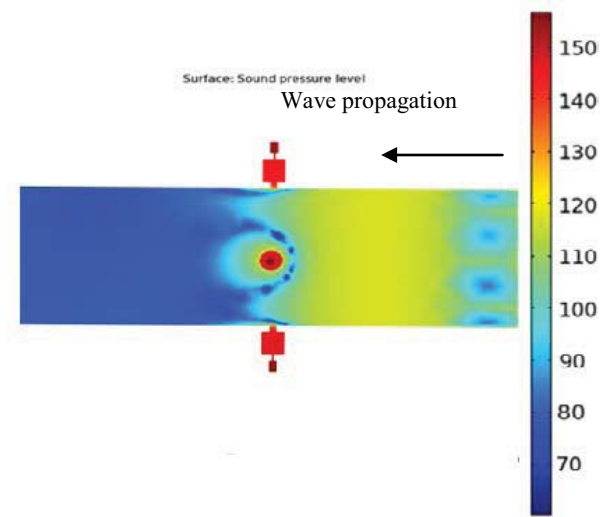
Figure 4.15 A closer view of Sound Pressure levels distribution at 2712 Hz on the surface of the pipe with and without 2 DOF designed resonators.

4.4 VALIDATION OF RESULTS

4.4.1 Numerical Validation

The Dual Resonators used by Selamet et al [10] was used as a benchmark test to validate the analytical design method described previously. The same dual resonator was used in COMSOL simulation to validate the level of transmission loss obtained analytically. Fig 4.2

The main duct was taken to have a square cross-section of 4.3cm x 4.3cm. The square main duct is then connected to a circular impedance tube with smooth transitions that retain a constant cross-sectional area development. The following figures show the results

53

of simulation as generated by COMSOL. The input frequency was varied and the acoustic response of the system was recorded.

As shown in fig 4.16, there is a noticeable reduction in noise levels. There is nearly a 20 dB decrease in noise levels at the 73Hz resonant frequency and a 25dB decrease in noise levels at the 166Hz resonant frequency. The noise response of the Dual Helmholtz Resonator versus frequency is shown plotted in Fig. 4.18. Using the stated equations for two DOF resonators the results match the analytically calculated values with an error of % 1.The transmission loss obtained numerically has negative values in the case when the resonators exhibit anti-resonance. This is evident from fig 4.18 in the range of 120 Hz to 175 Hz. The negative values of the sound pressure levels indicate that the reference pressure used for the computations is more than the measured sound pressure level which can be improved by decreasing the sound pressure levels. After generating and solving a a variety of meshes this solution was obtained where the analytical and the experimental values seem to be very close to each other Fig. 4.18..
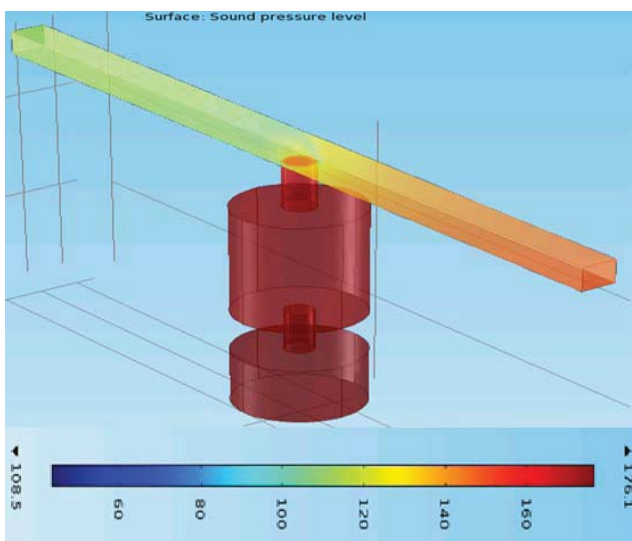
Figure 4.16 Sound Pressure levels at the resonating frequency 73 Hz.
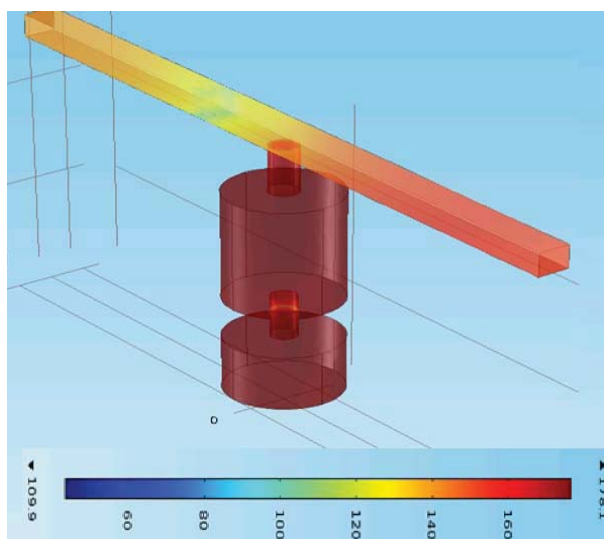
Figure 4.17 Sound Pressure levels at the resonating frequency 166 Hz.

4.4.2 Experimental Validation

The main duct has a square cross section and was connected to a circular impedance tube .The apparatus used in the experiments to measure the transmission loss is based on two-microphone technique applied on the impedance-tube setup [15].

Along with the random sound input, B&K 3550 multichannel analysis system has been used. Throughout the frequency range of interest, the reflection coefficient measured on the downstream side of the resonator was ensured, by an appropriate termination, to remain below 0.1 which translates to accurately measured transmission loss.

4.5 CONCLUSION

A new design procedure has been proposed and validated in this chapter for noise attenuation using Helmholtz resonators in pipelines. Applied to one and two of Helmholtz resonators, the designed models of resonators have been verified numerically using COMSOL. All analytical and numerical results were validated using experimental results from published data. Attenuation of around 40 db has been achieved which proves not only the efficiency of the proposed design procedure but also the straightforward method to dimension the resonators.
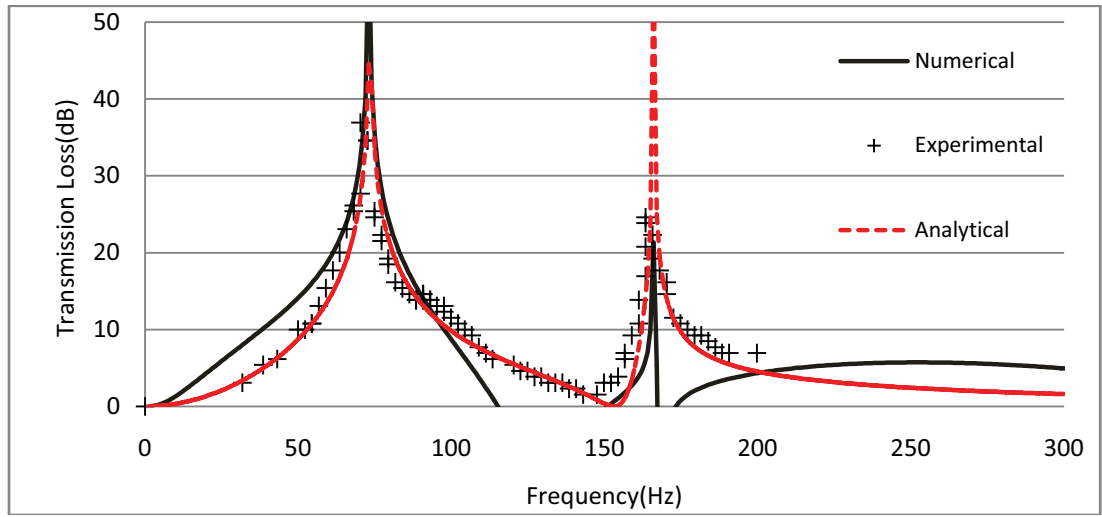
Figure 4.18 A comparison of Transmission Loss with published experimental results for a single 2 DOF resonator.

CHAPTER 5

SHAPE EFFECTS OF ONE DOF HELMHOLTZ

RESONATORS

5.1 INTRODUCTION

In this chapter the effect of geometry shape of the Helmholtz resonator on its resonant frequency and on its noise attenuation capability is discussed. The theory of resonant frequency depending on the shape of the vessel of the resonator is verified analytically and numerically using COMSOL for one and two degrees of freedom. The simulation was validated experimentally and has shown very good agreements. Various shapes of the resonators were compared in arrays. A better understanding of the shape effect is shown through simulations.

5.2 EXPERIMENTAL SET UP

Three different geometries of resonators were designed, modeled and manufactured using rapid prototyping process Fig 5.11,12,13. Due to some problems in the rapid prototyping set up the final prototypes of the spherical resonators had holes and therefore couldn't be used for the experiments A 100 mm pipe was also manufactured on which the conical and the cylindrical resonators were fixed and used for the experiments Fig 5.14 to Fig 5.16.

A preliminary test was made using a straight one meter pipe of PVC with no resonators to see the effect of natural damping due to the air itself. The pipe was attached to the insulation and mounted on a stand while the generated noise level was varied between 800 to 2000 Hz on one side of the pipe and similar level was collected on the other end, implying that there was little to no damping within the pipe. The four resonators were assembled on a polymeric part of pipe and attached in the middle of the main pipe cut in two parts using epoxy glue as shown in Fig 5.11 to Fig 5.13. Finally the duct tape was added as a precaution to hold it in place Fig 5.1 shows a picture of the experimental set up used for the test.

The aim was to find the range over which the resonator is effective along with the resonant frequency of the resonator and gives maximum noise attenuation. Initially the starting frequency was set at 800 Hz .The noise source was a speaker generating a sine wave with maximum SPL of 121 dB was verified and then the pipe was attached to the

noise source. A check was made along the pipe using the sound meter to identify any acoustic leakage. To verify any acoustic leakage, a noise measurement at the outlet was taken. A noise decrease of 2 dB was observed. Then the process was continued varying the frequency systematically, first increasing at regular intervals and then decreasing, whilst recording the sound level until the noise levels of the source were reached, and consequently no attenuation was found. This has established a range of values around which the resonator provided some level of attenuation. By varying the frequency it was found that the resonant frequency of the conical arrangement was nearly 840 Hz, around which a reduction of around 8 dB was observed. The noise level was found to be 106 dB. There was another check made using the noise level meter to check for acoustic leakages along the pipe and verify the source noise levels, and it was found that such leakages were completely negligible. Next was the testing of the cylindrical pipe arrangement. A similar sweep was performed using the sound meter to check for leakages and it was found that there were minor leakages around the connection region that might tamper with the experimental results. A sleeve made of cotton cloth was made to blanket the noise levels at these locations. The points of leakage were checked and it was found that the cotton cloth successfully blocked any acoustic leakage. On repeating the test for cylindrical resonators the resonant frequency was found to be around 1150 dB. The spherical case couldn't be tested since the spherical resonators had pores due to some defects in the rapid prototyping process during their manufacturing. The tests were also a part of Senior Design Project done by Mechanical Engineering students at King Fahd

University. They aided in the manufacturing of the resonators and procurement of the measuring instruments.

5.3 ONE DEGREE OF FREEDOM SIMULATIONS

A single 1 DOF cylindrical resonator was simulated numerically as shown in Fig. 4.4 and validated analytically in Fig 4.8. Both analytical and numerical simulation show good agreement. Numerical simulations have been performed for three various shapes of the resonator Cylindrical, conical and spherical. The following results were obtained with three different blade passing frequencies acting at the pipe inlet. The simulations show clear noise reduction for each shape depending on the BPF considered. Fig.5.2 shows four resonators mounted at the middle way of the pipe with clear reduction of sound
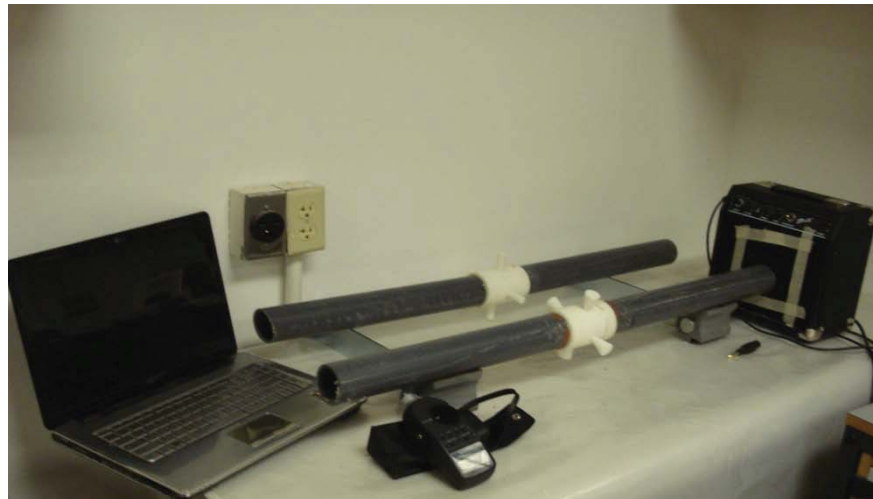

Figure 5.1 A picture of the experimental setup established to measure the noise attenuation offered by the modeled resonators

(>40dBA) using spherical resonators. They can achieve a transmission loss of around 35 dB which can visualized from the color of legend changing from dark orange to sky blue.. Fig 5.4 and Fig 5.6 depict the resonance phenomenon in cylindrical and conical resonators respectively. In order to have a clear view of the sound pressure level distribution in the pipes Fig 5.3, Fig 5.5 and Fig 5.7 can be referred to for spherical, cylindrical and conical geometries respectively. When comparing the results for the two configurations of arrays, i.e. one and four sets of one DOF resonators, the frequency for which they are designed don't match accurately showing a little difference of around 30-50 Hz. This happens because when array of resonators are put around their resonating frequencies some of them resonate for a particular value while others couldn't achieve full resonance for that value and this happens due to different orientations of the resonators and their slight misplacement around the sound carrying duct. This phenomenon can be perceived from Fig. 5.7, where different SPL are encountered for a particular designed frequency in the conical resonators.

Another notable feature, which can be visualized from Fig. 5.5 and Fig. 5.7, is the variation of sound pressure levels inside the resonators. The sound pressure levels of the resonators depends on the amount of noise absorbed by the respective chamber, i.e. the chamber which is tuned to the resonant frequency will absorb more amount of noise and will thereby exhibit higher sound pressure levels and vice versa .The amount of noise absorbed by the resonator also depends on their placement on the noise transmitting duct. If they are placed in regions where the crest of the wave falls, they will encounter more acoustic energy and hence, will absorb more sound pressure than the others.
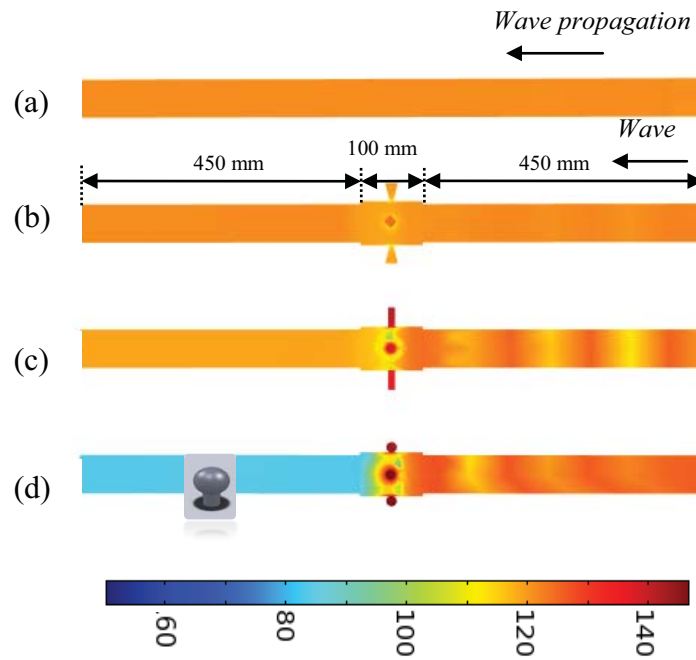
Figure 5.2 The sound pressure level at 1.284 kHz (a) Pipe without any resonators, (b) Pipe with conical resonators,(c) Pipe with cylindrical resonators, (d) Pipe with Spherical resonators(Spherical resonant frequency).
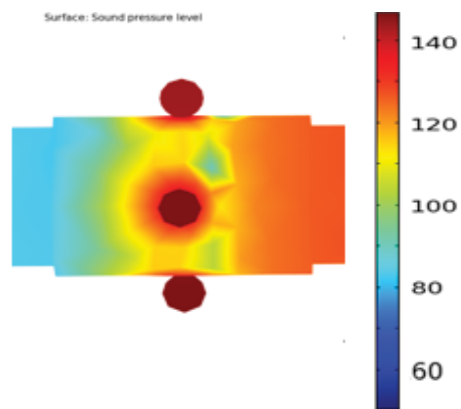
Figure 5.3 A closer view of the sound pressure level distribution at 1.284 kHz (Spherical resonant frequency).

63
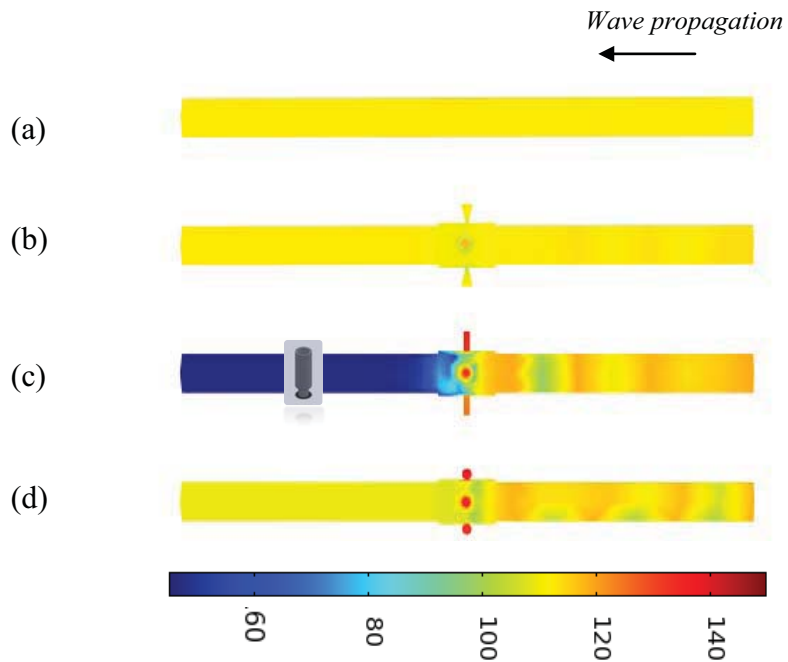
Figure 5.4 The sound pressure level at 1.15 kHz (a)Pipe without any resonators, (b) Pipe with conical resonators(c) Pipe with cylindrical resonators (Cylindrical resonant frequency), (d) Pipe with Spherical resonators.
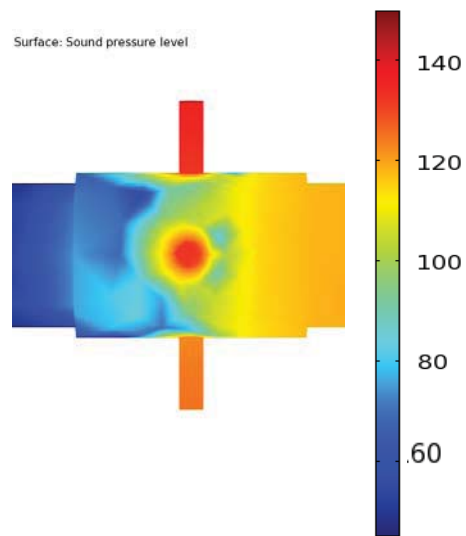
Figure 5.5 A closer view of the sound pressure level distribution at 1.15 кHz (Cylindrical resonant frequency).
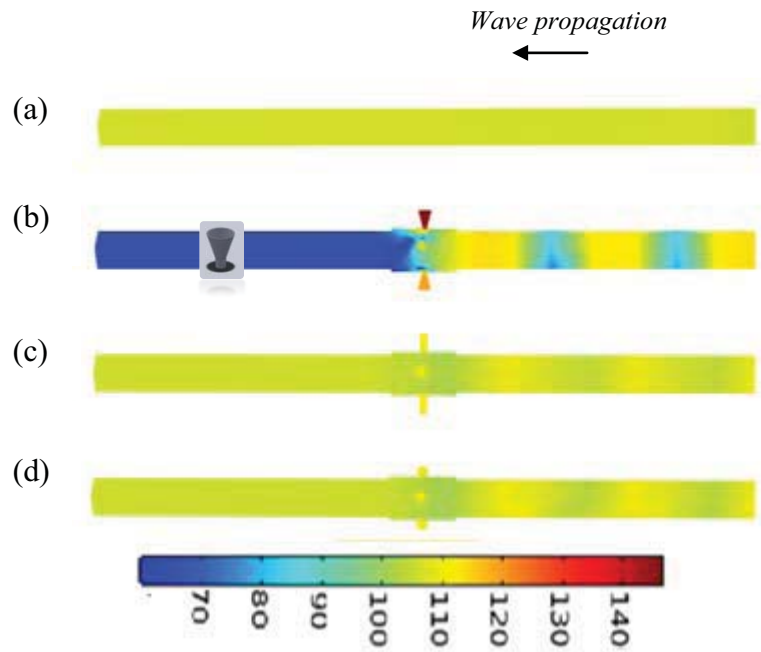
Figure 5.6 The sound pressure level distribution at 0.84 kHz (a)Pipe without any resonators (b) Pipe with conical resonators (Conical resonant frequency) (c) Pipe with cylindrical resonators (d) Pipe with Spherical resonators.
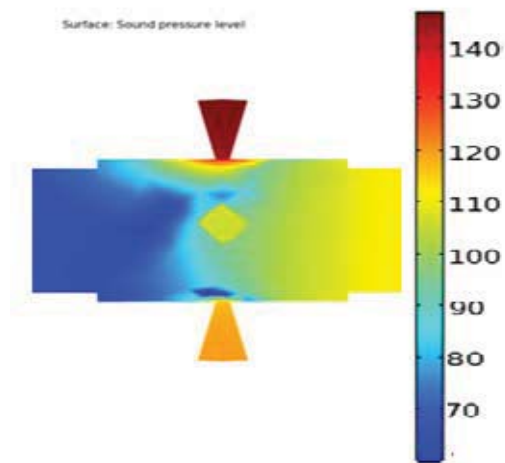
Figure 5.7 A closer view of the sound pressure level Distribution at 0.84 kHz (Conical resonant frequency)

5.4 EXPERIMENTAL RESULTS AND VALIDATION FOR ONE DOF RESONATORS

Fig 5.8 and Fig 5.9 show the resonator response over their effective ranges. An anti-resonance behavior was displayed at around 1200 Hz in cylindrical resonator arrangement and at around 930 in conical resonator arrangement which caused the noise level to amplify by around 3 dB. This phenomenon is not uncommon in such resonator arrangements. Every resonator possesses this phenomenon and at times is undesirable when the noise to be reduced is broad band noise. While the power source and the duct were same still a little shift is encountered in the frequencies for the two geometries Fig 5.8 and Fig 5.9 and the reasons attributed to this phenomenon are defects in the assembling of the manufactured pipes containing the resonators on the transmission pipe and incompetence of the experimental set up.
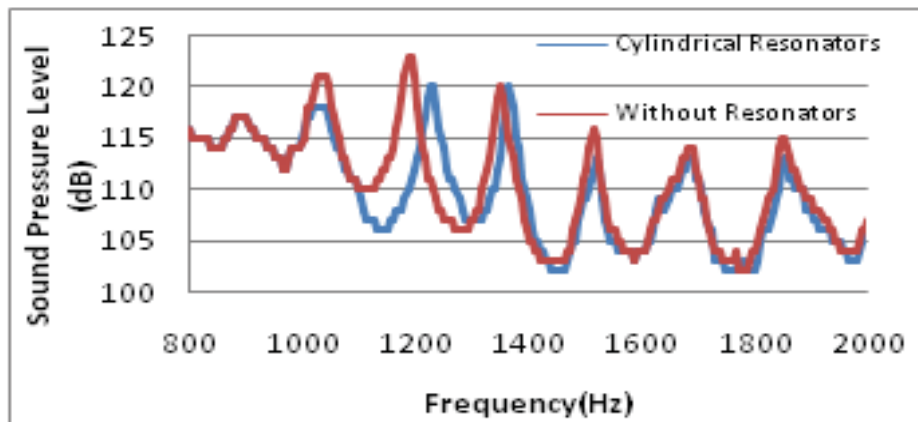
Figure 5.8 A comparison of the sound pressure levels from the experiments for a pipe fitted with an array of cylindrical resonators with a pipe without any resonator.
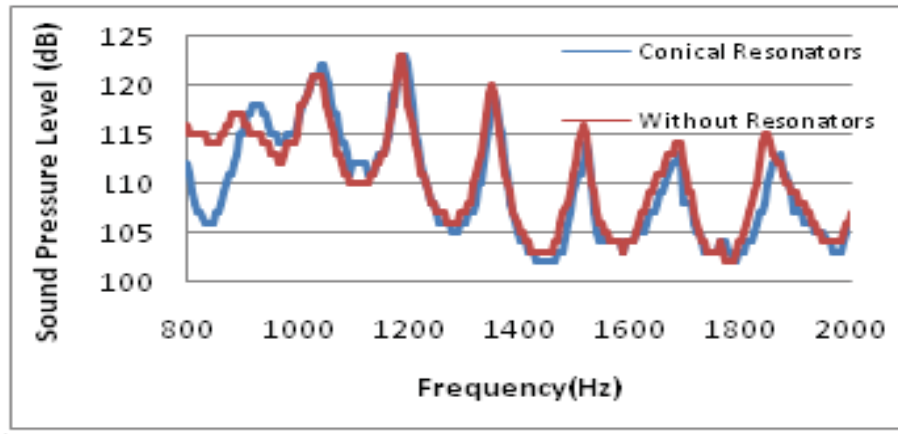
Figure 5.9 A comparison of the sound pressure levels from the experiments for a pipe fitted with an array of conical resonators with a pipe without any resonator.
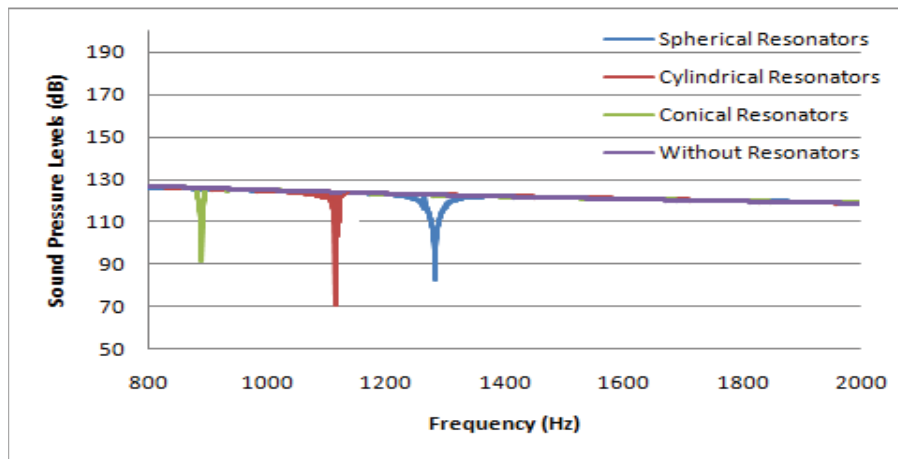
Figure 5.10 A comparison of the sound pressure levels from the simulations for a pipe fitted with three different arrays of resonators with a pipe without any resonator

Fig 5.10 represents a numerical comparison of the sound pressure levels of the three different geometries simulated. On careful consideration the resonant frequencies found for cylindrical and conical resonators from the experiments match closely with the frequencies found in the simulations. The resonators tuned to their resonant frequencies

67

are shown in fig 5.10, which can be correlated with the values obtained in the experiments.

The dimensions of the three different geometries were taken so as to have equal volumes which will lead to the same resonant frequency according to Eqn. (2.18).But from fig. 5.10 it is evident that all the three geometries exhibit different resonant frequencies which happened due to technical errors in the model's mesh generation. A variety of mesh was generated for the three different cases. The finer the mesh the better are the results On meshing the conical and the spherical resonators the generated mesh of the model exhibited a slight difference in the shape e.g. the conical shape transformed into a pyramid and the solution was done taking into account the shape of the pyramid Fig 5.7.When the ratio of volume of the meshed pyramid to the modeled conical geometry was taken, it comes out to be 0.75. This change in the volume of the geometry explains the changes in the resonant frequency of the three geometries governed by Eqn. (2.18). The mesh size was varied according to the accuracy and computability of the technical resources to get the desired results. The mesh size chosen for spherical was different from the other two geometries, hence, the resonating frequency of the three cases were found to be close but not equal.

The noise reduction achieved in the experiments are less than those achieved in the COMSOL simulations which could be due to following reasons: One dimensional propagation is assumed in the simulations which can be attenuated more easily than the actual three dimensional propagation in the experiments, improper acoustics terminations

at the open ends, damping offered by the polymeric material and the PVC pipe due their

acoustic absorption coefficients.
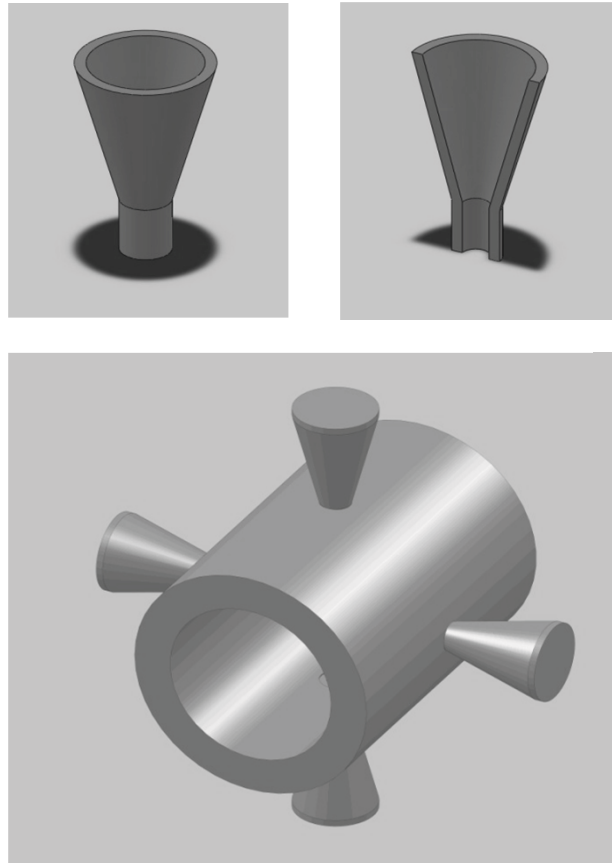
Figure 5.11 The Conical Resonators Arrangement
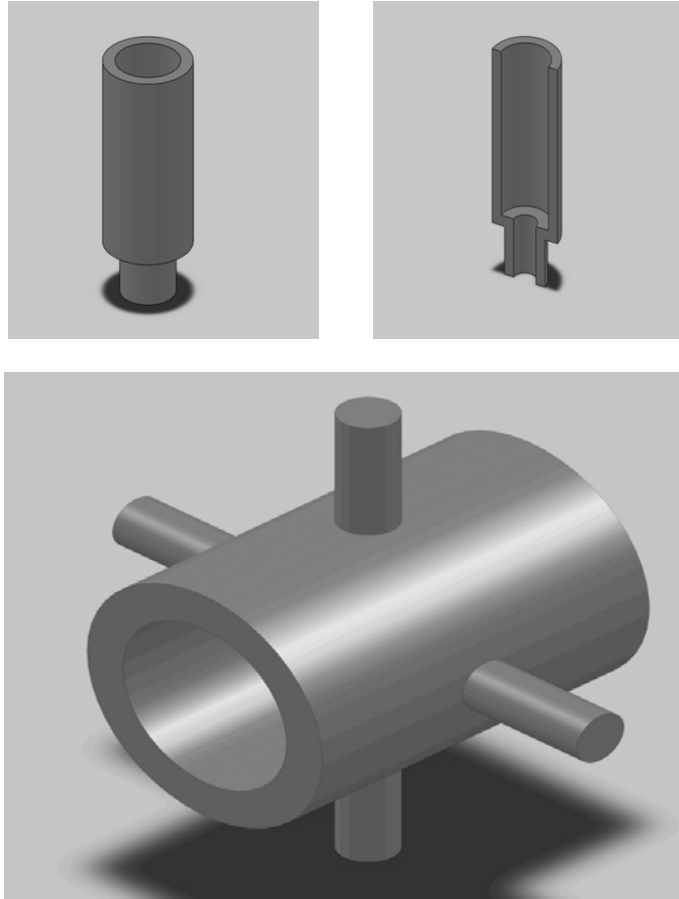
Figure 5.12 The Cylindrical Resonators Arrangement
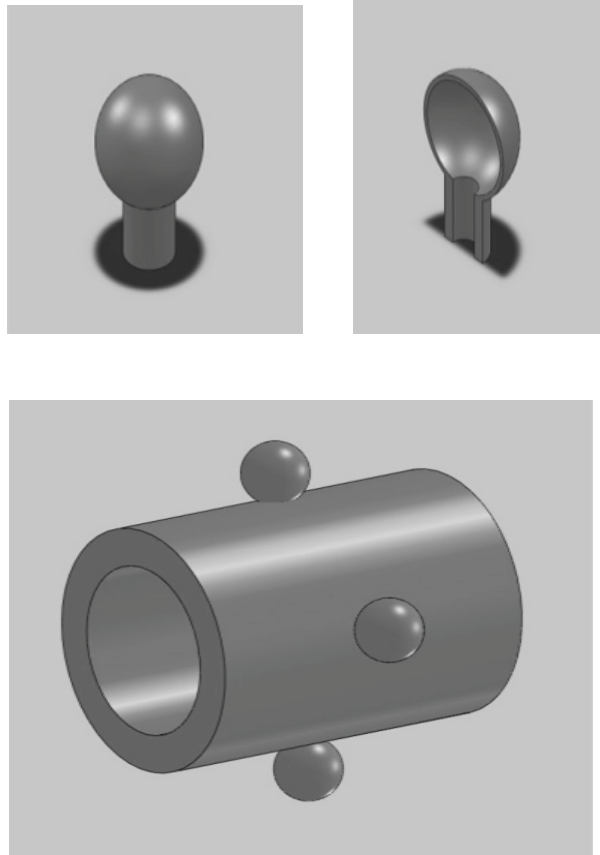
Figure 5.13 The Cylindrical Resonators Arrangement
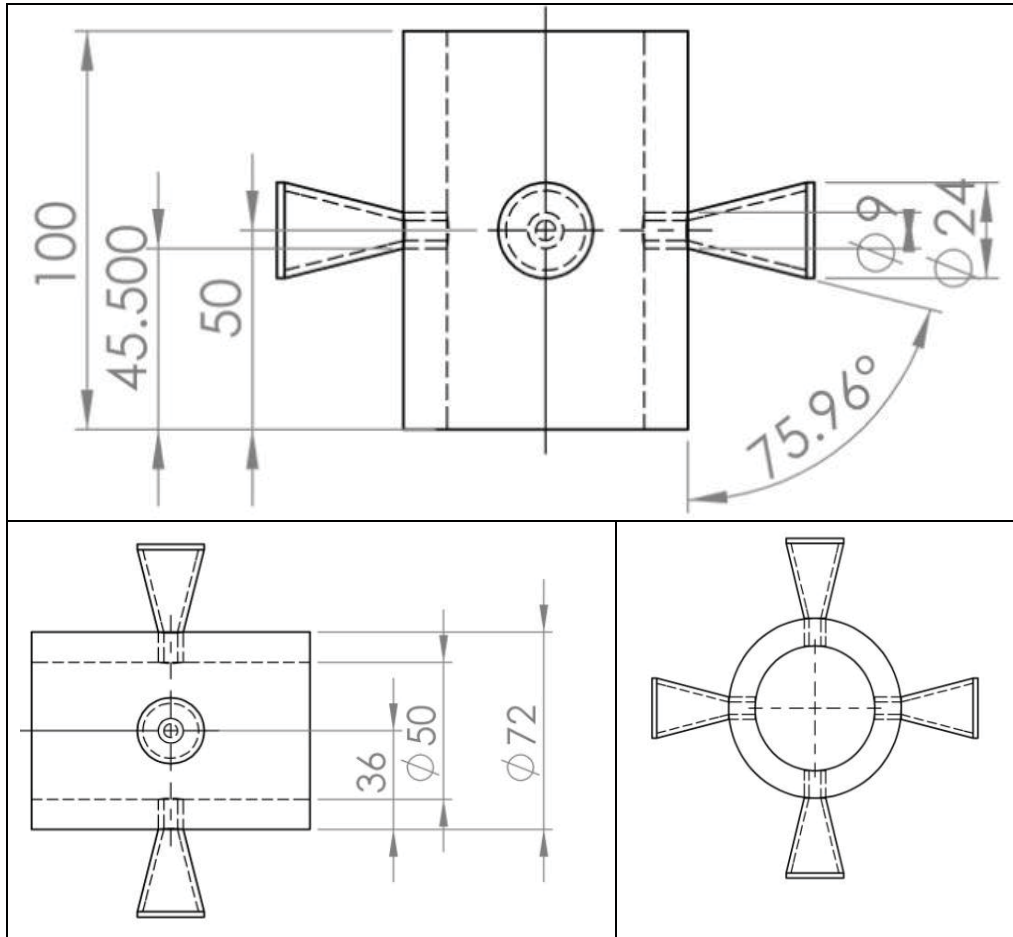
Figure 5.14 The Conical Resonators Arrangement drawings
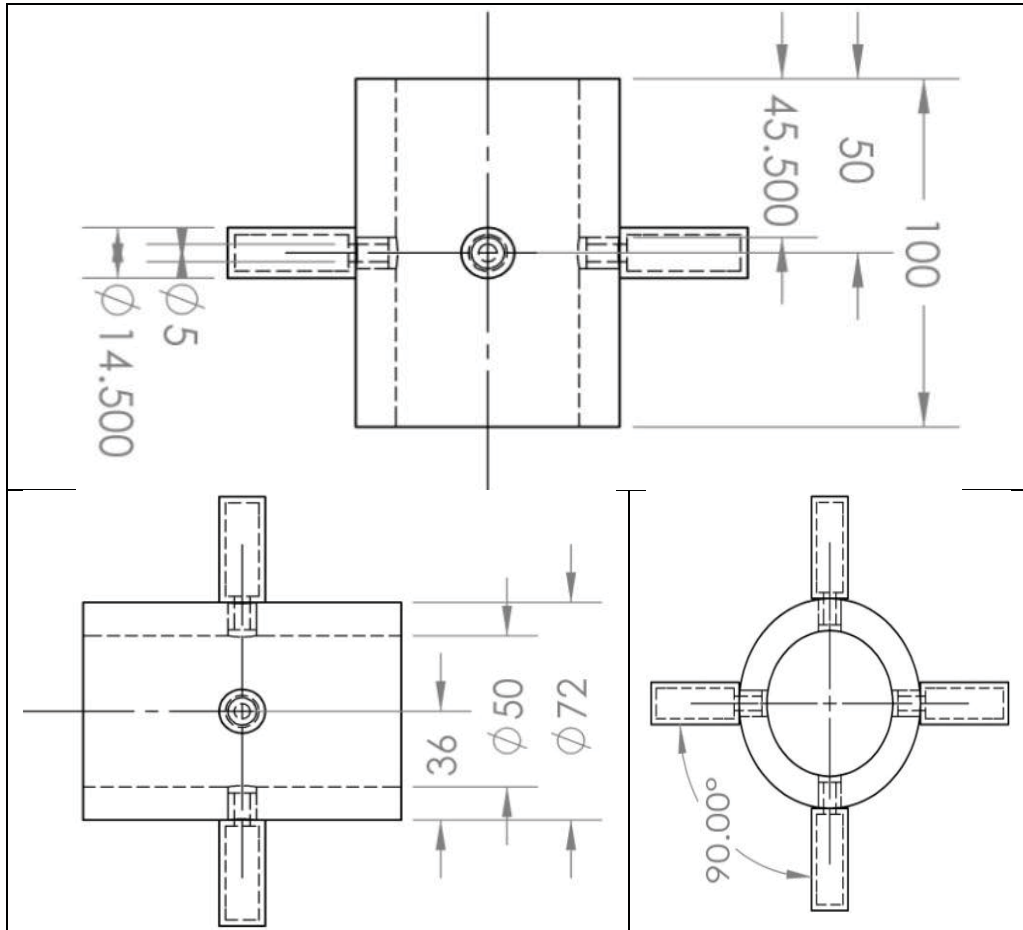
Figure 5.15 The Cylindrical Resonators Arrangement drawings
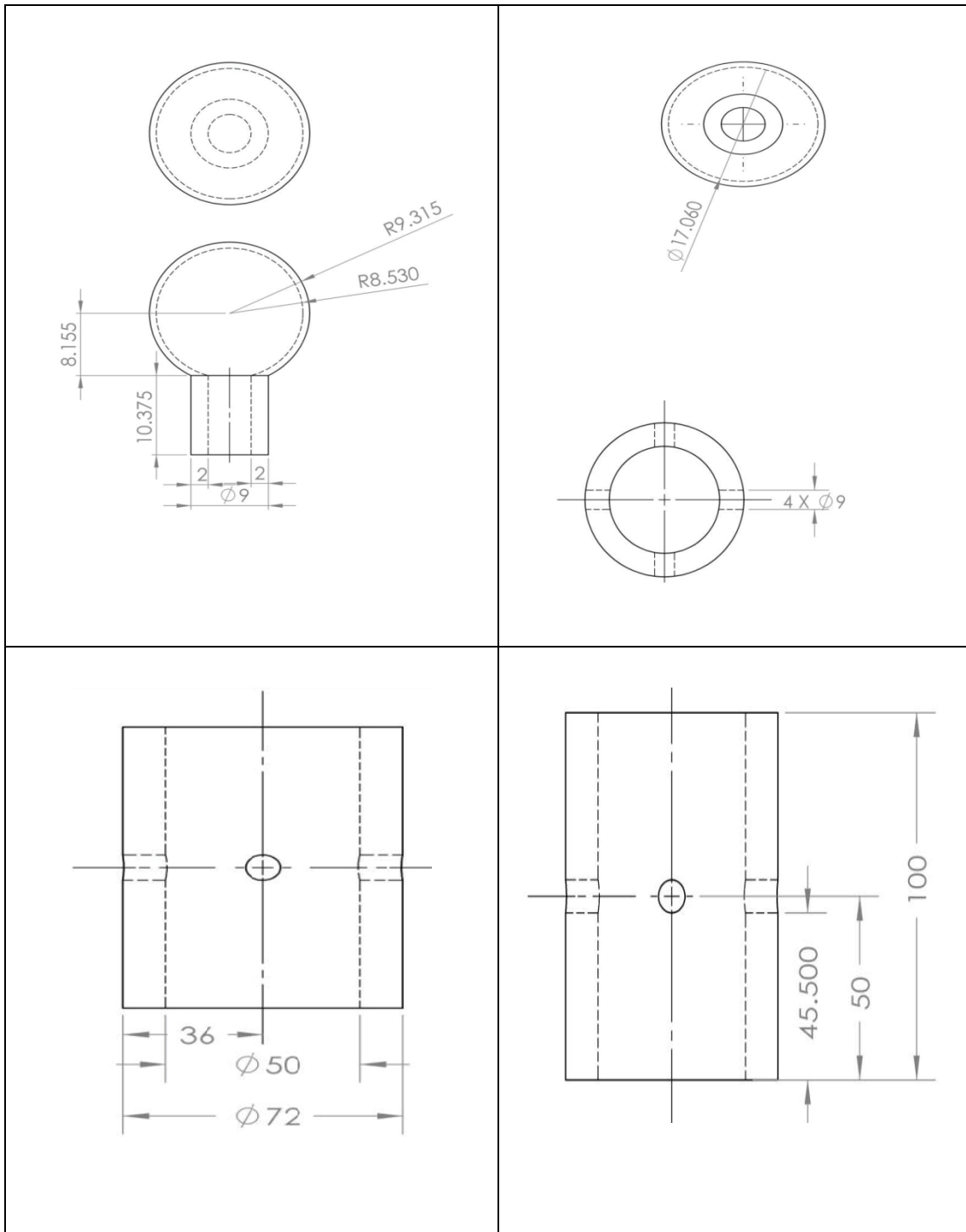
Figure 5.16 The Spherical Resonators Arrangement and the transmission pipeline drawings

5.5 CONCLUSION

A numerical simulation validated by experimental tests to estimate the level of noise attenuated using Helmholtz resonators as an add-on solution to pipeline has been presented in this chapter. The method was used to analyze the effects of the various shapes e.g. cylindrical, conical, and spherical on the noise reduction in pipelines.

Comparison tests between various shapes of the resonator have shown in both numerical and experimental methods that cylindrical resonators give better noise attenuation than the conical and the spherical resonators. The three different geometries have distinct resonant frequencies and transmission loss even though the volume for all the cases is equal. Some of the noted effects of number of resonators are when using one resonator the reduction of noise takes a while, but in the case of four resonators the reduction is almost instant. Also the increase in transmission loss achieved by increasing the number of resonators from one to four has a very limited effect range, increasing the transmission loss by around 5 dB.

CHAPTER 6

CONLUSIONS AND RECOMMENDATIONS

7.1 CONCLUDING REMARKS

This work has focused on getting a better reduction of noise generated from centrifugal compressors using the very old concept of Helmholtz Resonators, which would be used as an add on solution to this menace. The task is by no means complete, but all the theoretical models and design schemes can be used for designing Helmholtz resonators for a number of applications where noise reduction is required. Design of one and two Degree of freedom Helmholtz resonators for maximum possible noise reduction in ducts and pipelines based on real plant configuration could be done using this work.

Numerical simulations validated by experimental tests are used to estimate the level of noise attenuated using Helmholtz resonators .The add-on solution was also tested for the effects of the various shapes e.g. cylindrical, conical, and spherical on the noise reduction in pipelines also forms a part of this work.

Comparison tests between various shapes of the resonator have shown in both numerical and experimental methods that cylindrical resonators give better noise attenuation than the conical and the spherical resonators.

The acoustic performance of a Non-Homogeneous array One and Two degree of freedom Helmholtz resonator composed of two Helmholtz resonators in series (neck–cavity–neck– cavity) is also investigated. Closed-form relationships have been developed for transmission loss of both configurations of resonators by using Transfer Matrix Method considering one dimensional acoustic wave propagation. Comparisons of the transmission loss from the TMM method, a numerical method (FEM), and experiments from published work show a reasonable agreement.

7.2 ACCOMPLISHMENTS

The pertinent accomplishments are summarized below.

• Developed a design procedure for one and two degree of freedom Helmholtz Resonators for maximum transmission loss i.e. for maximum possible noise reduction.

• Developed a more general and accurate model for calculating transmission loss of one and two degree of freedom cylindrical Helmholtz Resonators using Transfer matrix method.

- Analyzed the geometry effects of the three different shapes of Helmholtz Resonators namely cylindrical, conical and spherical geometries and validation of the analysis experimentally and numerically.

7.3 RECOMMENDATIONS FOR FUTURE WORK

When compared with the results of FEM and experiments the analytical equations for transmission loss for different geometries are still not as accurate as equations for cylindrical resonators. It is obvious that manufacturing of resonators of complex shapes such as spherical and conical is not an easy job. Some of the results from FEM indicates that the there is a room for better transmission loss in those shapes.

Improved experimental configurations should be considered when identifying the resonant frequencies, and transmission loss. Particularly in the experiments th difference in the Sound Pressure Levels won't be much and distinguishing the resonant frequencies for resonators accurately won't be easy.

Smart acoustic resonators should be the next research topic. Our acoustic resonator does have a potential to be adaptive. The smart structure can be attached to one end of the resonator, and the smart acoustic resonator can be realized by means of adaptively changing the acoustic radiation impedance of the smart structure. Multiple holes also can be opened along the resonator like a flute, and the smart acoustic resonator can also be realized through adaptively adjusting opening or closing status of the holes. Different

sizes of sound absorbing materials can also be experimented and there by checked for the

noise attenuation for comparison purposes.

NOMENCLATURE

Symbol	Representation
c	Speed of sound
M_a	Acoustic mass of the resonator
C_a	Acoustic compliance
a	Radius of the neck
L	Actual neck length
p	pressure
T	temperature
L_{eff}	Effective neck length
V	Cavity volume of the Helmholtz resonator
F	Force applied
Q	Monopole source
q	Dipole Source
f	Resonant frequency
k	Wave Number
V_N	volume of the neck ($V_n = a_n \times l_n$)
V	Volume of the resonator without the neck
h	Height of the resonator from the bottom to the neck
L	Actual neck length
a_c	Cross sectional area of the cavity
a_n	Cross sectional area of the neck
L_{eff}	Effective neck length
V	Cavity volume of the Helmholtz resonator
l_c	Length of the cavity

Symbol	Representation
K	Stiffness of the mass-spring damper system
R_m	Damping Capacity of the mass damper system
R_a	Acoustic damping capacity of the resonator
M_m	Mass of the spring damper system
λ	Ratio of area of cross section in one DOF resonators
α	Ratio of first neck cross sectional area to neck length.
β	Ratio of second neck cross sectional area to neck length
ρ	Medium Density
γ	Ratio of Specific Heats
ω	Excitation frequency [Hz]
Z_r	Impedance of the resonators
A_{c1}, a_{n1}	Cross sectional area of the first neck
A_{c2}, a_{n2}	Cross sectional area of the second neck
l_{c1}, l_{n1}	Length of the first neck
l_{c2}, l_{n2}	Length of the second neck
f_1, f_2	First and second resonant frequencies
V_1, V_2	First and second Cavity volumes
a_{v1}, a_{c1}	Cross sectional area of the first cavity
a_{v2}, a_{c2}	Cross sectional area of the second cavity
l_{v1}, l_{v2}	Lengths of the first and the second cavity
l_n	Length of the neck
F_N	Area of the neck

APPENDIX

Appendix A

ONE DEGREE OF FEEDOM RESONATORS

The equation for angular resonating frequency of one degree of freedom resonator is given by [8]

$$\omega = c \sqrt{ -\frac{3.L_n + L_c \lambda}{2L_n{}^3} + \sqrt{\left(\frac{3.L_n + L_c \lambda}{2L_n{}^3}\right)^2 + \frac{3\lambda}{L_n{}^3 L_c}} } \qquad (A1)$$

Where

$$\lambda = \frac{a_n}{a_c}$$

a_n = cross section area of the neck

a_c = cross section area of the cavity

L_n = Corrected neck length

L_c = Length of the volume

c = speed of sound

Refer to Fig. 4.1 for correlating the dimensions. On solving equation (A1) for the two areas of cross sections one gets Eqn.(A2) and (A3),

$$a_n = \frac{a_c(-3.c^2.\omega^2.L_n.L_c - \omega^4.L_n^3.L_c)}{c^2(-3.c^2 + \omega^2 L_c^2)}$$

(A2)

$$a_c = \frac{a_n.c^2(-3.c^2 + \omega^2 L_c^2)}{(-3.c^2.\omega^2.L_n.L_c - \omega^4.L_n^3.L_c)}$$

(A3)

From these equations it is obvious that for getting positive real values of the two areas of cross sections the denominator should be negative for (A2) while the numerator should be negative for (A3). i.e.

$$-3.c^2 + \omega^2 L_c^2 < 0.$$

Hence, $\omega < \sqrt{\dfrac{3.c^2}{L_c^2}}$

This on solving for resonating frequency gives

$$f < \left(\frac{1}{2\pi}\sqrt{\frac{3.c^2}{L_c^2}} = 0.2756\frac{c}{L_c}\right)$$

83

Appendix B

TWO DEGREE OF FEEDOM RESONATORS

The equation for angular resonating frequency of one degree of freedom resonator is given by,

$$f_{1,2} = \frac{c}{2\sqrt{2}\pi}\sqrt{\left(\frac{\alpha}{V_1}+\frac{\beta}{V_1}+\frac{\beta}{V_2}\right)\pm\sqrt{\left(\frac{\alpha}{V_1}+\frac{\beta}{V_1}+\frac{\beta}{V_2}\right)^2-4\frac{\alpha}{V_1}\frac{\beta}{V_2}}}$$

(A4)

Where,

$$\alpha = \frac{a_{n1}}{l_{n1}} \text{ and } \beta = \frac{a_{n2}}{l_{n2}}$$

Which is derived from the equation [10]

$$f_{1,2} = \frac{c}{2\sqrt{2}\pi}\sqrt{\left(\frac{A_{C1}}{l'_{C1}V_1}+\frac{A_{C2}}{l'_{C2}V_1}+\frac{A_{C2}}{l'_{C2}V_2}\right)\pm\sqrt{\left(\frac{A_{C1}}{l'_{C1}V_1}+\frac{A_{C2}}{l'_{C2}V_1}+\frac{A_{C2}}{l'_{C2}V_2}\right)^2-4\frac{A_{C1}}{l'_{C1}V_1}\frac{A_{C2}}{l'_{C2}V_2}}}$$

(A5)

Refer Fig. 4.2 for correlating the dimensions. On solving the above equation for V_1 and V_2 i.e. volume of first and second cavity one gets Eqn. (A6) and (A7)

$$V_1 = \frac{(8.a_{n1}^2 a_{n2} c^4)}{l_{n1}\left(2a_{n1}a_{n2}c^2 f_1^2 + 2a_{n1}a_{n2}c^2 f_2^2 - \sqrt{\left(4a_{n1}^2 a_{n2}^2 c^4 f_1^4 - 8a_{n1}^2 a_{n2}^2 c^4 f_1^2 f_2^2 + 4a_{n1}^2 a_{n2}^2 c^4 f_2^4 - \frac{16a_{n1}a_{n2}^3 c^4 f_1^2 f_2^2 l_{n1}}{l_{n2}}\right)}\right)}$$

$$+ \frac{(8.A_{C1}A_{C2}^2 c^4)}{l_{n2}\left(2a_{n1}a_{n1}a_{n2}c^2 f_1^2 + 2a_{n1}a_{n2}c^2 f_2^2 - \sqrt{\left(4a_{n1}^2 a_{n2}^2 c^4 f_1^4 - 8a_{n1}^2 a_{n2}^2 c^4 f_1^2 f_2^2 + 4a_{n1}^2 a_{n2}^2 c^4 f_2^4 - \frac{16a_{n1}a_{n2}^3 c^4 f_1^2 f_2^2 l_{n1}}{l_{n2}}\right)}\right)}$$

(A6)

$$V_2 = \left[\frac{0.5\left((a_{n1}a_{n2}c^2)(2f_1^2 + 2f_2^2) - \sqrt{\left(a_{n1}^2 a_{n2}^2 c^4 (2f_1^2 + 2f_2^2)^2 - \dfrac{16a_{n1}a_{n2}^2 c^4 f_1^2 f_2^2 (a_{n2}l_{n1} + a_{n1}l_{n2})}{l_{n2}} \right)} \right)}{f_1^2 f_2^2 (a_{n2}l_{n1} + a_{n1}l_{n2})} \right]$$

<div align="right">(A7)</div>

The two volumes V_1 and V_2 are real if the expressions under the square root are positive or nil. Hence, a new condition emerges and is given below

$$\left(\frac{f_1^2}{f_2^2} + \frac{f_2^2}{f_1^2} \right) \geq 2\left(1 + \frac{2a_{n2}l_{n1}}{a_{n1}l_{n2}} \right)$$

<div align="right">(A8)</div>

Which can also be written as,

$$\left(\frac{f_1^2}{f_2^2} + \frac{f_2^2}{f_1^2} \right) \geq 2\left(1 + \frac{2\gamma_a}{\gamma_l} \right)$$

Where,

$$\gamma_a = \frac{a_{n2}}{a_{n1}} \text{ and } \gamma_l = \frac{l_{n2}}{l_{n1}}$$

MATEHMATICA CODES FOR ONE AND TWO DEGREE OF

FREEDOM RESONATORS TRANSMISSION LOSS

One Degree of Freedom Resonators

```
S=Ap;
Z1=c/S;
As1=Cos[k*Ln];
As2=Cos[k*Lc];
Ds1=Cos[k*Ln];
Ds2=Cos[k*Lc];
Bs1=i*c*Sin[k*Ln]/An;
Bs2=i*c*Sin[k*Lc]/Ac;

Cs1=i*An*Sin[k*Ln]/c;
Cs2=i*Ac*Sin[k*Lc]/c;

Mr1=({
   {As1, Bs1},
   {Cs1, Ds1}
  });
Mr2=({
   {As2, Bs2},
   {Cs2, Ds2}
  });
Mrf=Mr1.Mr2;
zhr=Mrf[[1,1]]/Mrf[[2,1]];


Mr=({
   {1, 0},
   {1/zhr, 1}
  });
A1=Cos[k*L1];
B1=i*c*Sin[k*L1]/(S);
C1=i*S*Sin[k*L1]/(c);
D1=Cos[k*L1];
A2=Cos[k*L2];
B2=i*c*Sin[k*L2]/(S);
C2=i*S*Sin[k*L2]/(c);
```

```
D2=Cos[k*L2];
pi=Pi;
M11=({
   {A1, B1},
   {C1, D1}
  });
M22=({
   {A2, B2},
   {C2, D2}
  });
n=3
Table[M11=M11.Mr;M22=M11.M22;M11=M22,{n,3}]
TL=20*Log10[Abs[(M11[[1,1]]+(Z1*M11[[2,1]])+(M11[[1,2]]/Z1)+M11[[2,2]])/2]]
FullSimplify[TL]
```

Two Degree of Freedom Resonators

```
Z1=c/S;
As1=Cos[k*Ln1];
As2=Cos[k*Lc1];
As3=Cos[k*Ln2];
As4=Cos[k*Lc2];
Ds1=Cos[k*Ln1];
Ds2=Cos[k*Lc1];
Ds3=Cos[k*Ln2];
Ds4=Cos[k*Lc2];
Bs1=i*c*Sin[k*Ln1]/An1;
Bs2=i*c*Sin[k*Lc1]/Ac1;
Bs3=i*c*Sin[k*Ln2]/An2;
Bs4=i*c*Sin[k*Lc2]/Ac2;
Cs1=i*An1*Sin[k*Ln1]/c;
Cs2=i*Ac1*Sin[k*Lc1]/c;
Cs3=i*An2*Sin[k*Ln2]/c;
Cs4=i*Ac2*Sin[k*Lc2]/c;
Mr11=({
   {As1, Bs1},
   {Cs1, Ds1}
  });
Mr22=({
   {As2, Bs2},
   {Cs2, Ds2}
  });
```

```
Mr33=({
   {As3, Bs3},
   {Cs3, Ds3}
   });
Mr44=({
   {As4, Bs4},
   {Cs4, Ds4}
   });
Mrf1=Mr11.Mr22.Mr33.Mr44;
zhr1=Mrf1[[1,1]]/Mrf1[[2,1]];
A1=Cos[k*L1];
B1=i*c*Sin[k*L1]/(S);
C1=i*S*Sin[k*L1]/(c);
D1=Cos[k*L1];
M1=({
   {A1m, B1m},
   {C1m, D1m}
   });
Mr1=({
   {1, 0},
   {1/zhr1, 1}
   });
M=M1.Mr1.M1;

TL=20*Log10[Abs[(M[[1,1]]+(Z1*M[[2,1]])+(M[[1,2]]/Z1)+M[[2,2]])/2]]
FullSimplify[TL]
```

REFERENCES

[1] Liu Z.and. Kuzdzal M.J. ,*Noise Control Of An 11,000 Horsepower Single Stage Pipeline Centrifugal Compressor*, Proceedings of ASME Turbo Expo 2007 Power for Land, Sea, and Air, May 11, 2007

[2] Liu Z.and. Kuzdzal M.J., *Noise Reduction Of A Multistage Export / Reinjection Centrifugal Compressor Through The Use Of Duct Resonator Arrays*, 2002 Dresser-Rand Company Olean USA.

[3] Raitor T., Nise W., *Sound generation in centrifugal compressors*, 2008,Journal of Sound and Vibration, Volume 314, Issues 3-5, 22 July Pages 738-756

[4] Tang PK, Sirignano WA. *Theory of generalized Helmholtz resonator*. 1973,Journal of Sound and Vibration 26:247–62.

[5] Neise W., Koopmann G.H., *Reduction of centrifugal fan noise by use of resonators*, 1980,Journal of Sound and Vibration, Volume 73, Issue 2, 22 November, Pages 297-308

[6] Jeung K., Imdad I. "*Compressor Noise Attenuation Using Branch Type Resonator*". 1990.,Patent 4,927,342. May 22,

[7] Selamet A, Radavich PM, Dickey NS, Novak JM. *Circular concentric Helmholtz resonators.* 1997,Journal of Acoustical Society of America;101:41–51.

[8] Li, D. . *Vibroacoustic behaviour and noise control studies of advanced composite structures.* 2003,PhD thesis, University of Pittsburgh.

[9] Wan DM, Soedel DT. *Two degree of freedom Helmholtz resonator analysis*. 2004,SAE 2004-01-0387.

[10] Xu M.B., Selamet A., Kim H., *Dual Helmholtz resonator*, 2010,Applied Acoustics, Volume 71, Issue 9, September, Pages 822-829

[11] Ingard, U., ''*On the theory and design of acoustic resonators*,'' 1953,Journal of Acoustical Society of America 25, 1037–1061.

[12] Munjal M.L., *Acoustics of Ducts and Mufflers With Application to Exhaust and Ventilation System Design,* 1987,John Wiley and Sons,

[13] Dickey NS, Selamet A., Helmholtz *resonators: one-dimensional limit for small cavity length-to-diameter ratios.* 1996,Journal of Sound and Vibration,; 195:512–7.

[14] Khelladi, S. "*Predicting tonal noise from a high rotational speed centrifugal fan*", 2008,Journal of Sound and Vibration.

[15] Selamet A, Dickey NS, Novak JM. *The Herschel-Quincke tube: a theoretical, computational, and experimental investigation*. 1994,Journal of Acoustical Society of America;96:3177–85.

[16] Lee, C.M "*A modified transfer matrix method for prediction of transmission loss of multilayer acoustic materials*", 2009,Journal of Sound and Vibration.

[17] Hyoun-Jin Sim. "*Design of the intake system for reducing the noise in the automobile using support vector regression*", 2008,Journal of Mechanical Science and Technology.

[18] Charles W. Schmidt- "*Spheres of Influence - Noise that Annoys*" 2005, *Environmental health perspectives* • Volume 113 Number 1 January

[19]   Rayleigh JWS. *The theory of sound. 2nd revised and enlarged.* 1945,New York: Dover;.

[20]   Davis DD, Stokes GM, Moore D, Stevens GL. *Theoretical and experimental investigation of mufflers with comments on engine-exhaust muffler design.* 1954.

[21]   Alster M. *Improved calculation of resonant frequencies of Helmholtz resonators.* 1972,Journal of Sound and Vibration;24:63–85.

[22]   Panton RL, Miller JM. *Resonant frequencies of cylindrical Helmholtz resonators.* 1975,Journal of the Acoustical Society of America;57:1533–5.

[23]   Selamet A, Dickey NS, Novak JM. *A theoretical, computational, and experimental investigation of Helmholtz resonators with fixed volume: lumped versus distributed analysis.* 1995,Journal of Sound and Vibration;187:358–67.

[24]   Selamet A, Ji ZL. *Circular asymmetric Helmholtz resonators.* 2000, Journal of the Acoustical Society of America;107:2360–9.

[25]   Selamet A, Lee I-JOURNAL *Helmholtz resonator with extended neck.* 2003, Journal of the Acoustical Society of America;113:1975–85.

[26]   Selamet A, Xu MB, Lee I-J, Huff NT. *Helmholtz resonator lined with absorbing material.* 2005, Journal of the Acoustical Society of America;117:725–33.

[27]   Tang SK. *On Helmholtz resonators with tapered necks.* 2005,Journal of Sound and Vibration;279:1085–96.

[28]   Griffin S, Lane SA, Huybrechts S. *Coupled Helmholtz resonators for acoustic attenuation.* 2001,Journal of Sound and Vibration;123:11–7.

[29] Wan DM, Soedel DT. *Two degree of freedom Helmholtz resonator analysis.* 2004,SAE ,2004-01-0387.

[30] De Bedout JM, Franchek MA, Bernhard RJ, Mongeau L. *Adaptive-passive noise control with self-tuning Helmholtz resonators.* 1997, Journal of Sound and Vibration;202:109–23.

[31] Ji ZL, Ma Q, Zhang ZH. *Application of the boundary element method to predicting acoustic performance of expansion chamber mufflers with mean flow.* 1994, Journal of Sound and Vibration;173:57–71.

[32] Morse, P. M. and Ingard, K. U. *Theoretical Acoustics*. 1968,.New York: McGraw

[33] Kinsler, L. E., Frey A. R., Coppens A. B. and Sanders J. V.. *Fundamentals of Acoustics*, 1982,3rd revised edition. New York: John Wiley.Hill.

[34] Bell L. and Bell D., *Industrial Noise Control*, Second edition revised and expanded Dekker Inc, New York

[35] Sun H., Shin H., Lee S., Analysis and optimization of aerodynamic noise in a centrifugal compressor, 2006, Journal of Sound and Vibration 289 (2006) 999–1018

[36] Bies D., Hansen C., *Engineering Noise control, Theory and Practice,* Spon press London and New york

[37] Rice E J., *Propagation of waves in an acoustically lined duct with a mean flow*. 1969 NASA SP-207,345-355.

[38] Eversman W. *The effect of Mach number on the tuning of an acoustic lining in a flow duct*. 1970,Journal of the Acoustical Society of America 48,425-428

[39] . Doak E. And Vawya P. G., *Attenuation of plane wave and higher order mode sound propagation in lined ducts.* 1970, Journal of Sound and Vibration 12,201-224.

[40] Harel P. And Perulli M. *The influence of a stationary uniform axial flow on the propagation of acoustic modes of vibration in a cylindrical duct.* 1971, Journal of Sound and Vibration 15,455-474.

[41] Ko S. *Sound attenuation in lined rectangular ducts with flow and its application to the reduction of aircraft engine noise.* 1971,Journal of the Acoustical Society of America 50, 1418-1432

[42] Benzakein M., Kraft R. And Smith E, *Sound attenuation in acoustically treated turbomachinery ducts.* 1969 ASME 69- WA/GT-11

[43] Fischer F. and Andersson A., *Optimization of duct linings for sound attenuation.* 1969 The Boeing Company Report D*6-29356TN.*

[44] Prwmore-Brown C., *Sound propagation in a fluid flowing through an attenuating duct.* 1958, Journal of Fluid Mechanics 4, 393-406.

[45] Tack D. H. And Lambert F. F.,*Influence of shear flow on sound attenuation in lined ducts.* 1965 Journal of the Acoustical Society of America 38,655-666.

[46] Mungur P., Gladwell G. M. L., *Acoustic wave propagation in a sheared fluid contained in a duct.* 1969, Journal of Sound and Vibration 9,28-48.

[47] Mungur P. And Plljmblw H.. *Propagation and attenuation of sound in a soft walled annular duct containing a sheared flow*. 1969, NASA SP-207,305-327

[48] Kurze U. And Allen C., *The influence of flow and high sound pressure levels on the attenuation in a lined duct.* 1969 Bolt, Beranck and Newman, Inc. Progress Report No. 4.

[49] Shankar P., *On acoustic refraction by duct shear layers.*, 1971, Journal of Fluid Mechanics 47,s 1-91.

[50] Eversman W., *Effect of boundary layer on the transmission and attenuation of sound in an acoustically treated circular duct.* 1971, Journal of the Acoustical Society of America 39,1372-l 380.

[51] Ko S., *Acoustic-wave attenuation in lined rectangular ducts with uniform flow and shear flow.* 1971 The Boeing Company Report 06-25485.

[52] Mariano S., *Effect of a wall shear layer on the sound attenuation in acoustically lined rectangular ducts.* 1971, Journal of Sound and Vibration 19,261-275.

[53] Hersh A. S. And Catton I., *Flow duct testing of acoustic lining circular test section.* 1969 The Boeing Company Report 03-8036-6. 1971 Journal of the Acoustical Society of America 50, 992-1003D.

[54] Ring W. M. *Energy flux in duct flow.* 1971 ,Journal of Sound and Vibration 18,101-109

[55] The Fletcher-Munson curves, *www.wikipedia.com*

[56] Decibel range chart *www.helpcharts.com*

[57] Elden F. Ray Industrial noise series *Modeling Sound propagation* ,2010

VITAE

- Maaz Farooqui

- Born in Gorakhpur, India on Feb 06, 1987.

- Received Bachelor of Technology in Mechanical Engineering from Faculty of Engineering and Technology, Jamia Millia Islamia, India in 2009.

- Joined King Fahd University of Petroleum and Minerals in February, 2010 as a Research Assistant in Mechanical Engineering Department.

    Contact details:

    - **Present Address:** King Fahd University of Petroleum and Minerals, PO Box # 8664, Dhahran 31261, Kingdom of Saudi Arabia.

    - **E-mail Address:** g200905470@kfupm.edu.sa

    - **Permanent Address:** Abwam School, Barbarehna, Ghazipur, Uttar Pradesh, 233001, India

    - **E-mail Address:** maazfarooqui@gmail.com